# Performance of a novel structural insulated panel in tropical climates: experimental and numerical studies

**Thanongsak Imjai[*,1], Fetih Kefyalew[1], Reyes Garcia[2], Boksun Kim[3], Ana Bras[4], and Piti Sukontasukkul[5]**

[1]School of Engineering and Technology, Walailak University, Nakhon Si Thammarat, 80160, Thailand
[2]Civil Engineering Stream, School of Engineering, The University of Warwick, Coventry, CV4 7AL, UK
[3]School of Engineering, Computing and Mathematics, University of Plymouth, PL4 8AA, Plymouth, UK
[4]School of Civil Engineering and Built Environment, Liverpool John Moores University, Liverpool, L3 5UG, UK
[5]Department of Civil Engineering, Faculty of Engineering, King Mongkut's University of Technology North Bangkok, Bangkok, Thailand

**Corresponding author's e-mail: thanongsak.im@wu.ac.th*

## Abstract

This article investigates experimentally and numerically the thermal performance of a new type of structural insulated panel (SIP) termed 'UWall'. The panel core consists of an ad-hoc waffle skeleton of Expanded Polystyrene (EPS), EPS beads mixed with cement mortar (Portland cement type I and recycled concrete aggregate), and two external water-proof cement boards. The experimental programme examined the panels in three Phases. In Phase 1, 200×200×100 mm block specimens were exposed to a temperature of 70°C for 12 hrs. It was found that the new UWall specimens had a better thermal performance (by up to 20%) over other types of walls typically used in house construction in Southeast Asia such as mon block wall. In Phase 2, five scaled-down house units (1.5×1.5×2.8 m) were built in Southern Thailand. Temperature and relative humidity outside/inside the units were continuously monitored for 7 days during the summer season. It was found that the new UWall has a good thermal resistance by reduced outdoor temperatures by up to 4°C compared to mon-block wall material. The house units were subsequently modelled in Abaqus® software, and the modelling approach proved accurate (within 10%) at simulating the thermal performance of the house units. UWall panels were also tested in bending to determine their structural capacity. It was found that the panels can be safely used as load-bearing walls for single-storey houses. Design charts are then proposed and used to design and build a full-scale house in Phase 3. In Phase 3, a 10×7 m full-scale single-storey house was built using the new UWall panels. Based on results from bioclimatic charts, it was found that daytime temperature and humidity in the full-scale house were deemed as uncomfortable. However, if air movement was provided, the house remained within the comfortable zone at all times. New design charts for full-scale houses with UWall are proposed to meet a desired user-comfort level. This study is expected to promote the use of SIPs in house construction in tropical climates, which in turn is envisaged to save energy and make construction more sustainable.

**Keywords:** Structural insulated panels; Thermal performance; Finite element analysis; Bending tests; Full-scale testing; Tropical climates.

## 1. Introduction

Southeast Asia enjoys a hot and humid tropical climate practically all year round. However, for the last decades, the region has also proven to be extremely vulnerable to climate change. Particularly in Thailand, the maximum recorded temperatures rose from 38º-41ºC to 42º-44ºC in the period 2001-2016 [1]. Thailand also has a high average relative humidity (RH) of around 70-80%. The wind speed is relatively low, with a reported annual average speed of 5.0 m/s [2]. This weather conditions often lead to thermal discomfort in buildings and houses around the country. As a result, building occupants make intensive use of air conditioning, thus leading to increasing energy consumption. In buildings, the occupants' comfort is affected by various environmental variables including the air temperature, solar radiation, indoor air quality/speed and RH [3, 4], among others. However, the type of construction and materials used in construction can also have a significant impact on thermal comfort of occupants. For this reason, the construction industry in Southeast Asia is trying to find alternative construction materials to increase thermal comfort (and in turn reduce energy consumption) in buildings and houses.

In typical building and houses, walls have the largest exposed area of all structural/architectural components. Sunlight and warm air heat the external walls (most of which are built with masonry), and such heat is stored and eventually released into the building. As a result, the improvement of the thermal performance and insulation of walls is often seen as a feasible solution to improve the occupants' comfort [5-7]. In recent years, different materials and systems have been proposed to improve the thermal performance of walls. For instance, Phase Change Materials (PCMs) have proven effective at improving the thermal comfort of occupants and at reducing energy consumption in buildings [8-15]. In PCMs, the change of material state leads to heat retention during melting, and to heat release during hardening. However, research has shown that, compared to conventional concrete walls with PCMs, composite walls have a better energy storage, which leads to an improved thermal inertia as well as to lower indoor temperatures in buildings [16-21].

In recent years, structural insulated panels (SIPs) have been extensively used in house construction due to their fast installation, cost-effectiveness and good insulation properties. Whilst studies [22-24] have shown that SIPs can effectively be used indoors, they require waterproof membrane sheets for outdoor use, which increases the cost of SIPs [7]. This has limited the use of SIPs in the construction of houses in Southeast Asia. To bypass this issue, the authors have recently developed a new type of SIP (termed 'UWall' in this article) suitable for outdoor use [6]. The new SIP is particularly suitable for rapid construction of buildings and housing units. To date, however, the structural and thermal performance of the new UWall SIP has not been assessed under real environmental conditions. Moreover, recent studies [25, 26] identified a lack of research showing the effectiveness of SIPs in actual full-scale buildings and houses. These tests are necessary before the new UWall SIP can be adopted in real construction projects.

This article investigates experimentally and numerically the thermal performance of the new UWall SIP. The UWall SIPs consists of cement boards, foamed concrete, and an Expanded Polystyrene (EPS) waffle panel that together provide a better thermal as well as structural performance over existing construction practices. The experimental programme was divided into three Phases.

- Phase 1: small (200×200×100 mm) concrete blocks were tested to assess the thermal behaviour of different types of walls and plastering materials, including the new UWall SIP.
- Phase 2: prototype UWall SIPs (600×2800 mm) were tested under combined axial and bending up to failure. Likewise, scaled-down house units were also built with UWall SIPs to assess their thermal performance in a tropical climate (Southern Thailand).
- Phase 3: examines the performance of a full-scale house built with new UWall SIPs. The analysis is based on ISO 7730 guidelines [27, 28].

Finite element analyses (FEA) were also performed on the different structural elements to further examined their thermal performance. This article contributes towards promote the use of SIPs in cooperated use of recycled concrete aggregate in house construction in tropical climates, which in turn is envisaged to save energy and make construction more sustainable.

## 2. Methodology

### 2.1. Phase 1: Thermal tests on wall systems

Initial tests were carried out on 200×200×100 mm (height×length×thickness) specimens to examine the thermal performance of different wall systems. The wall systems considered here are representative of those widely used in house construction across Southeast Asia. The following seven wall systems were tested in Phase 1:

- Mon block [29]: one control specimen (w1-c), and one plastered specimen (w1-p).
- Brick block [30]: one control specimen (w2-c), and one plastered specimen (w2-p).
- Light weight (LW) block [31]: one control specimen (w3-c), and one plastered specimen (w3-p).
- Composite infill wall [32]: three specimens (w4)
- SIP with polyurethane (PU SIP): three specimens (w5)
- SIP with expanded polystyrene (EPS SIP): three specimens (w6)
- UWall SIP: three specimens (w7)

Fig. 1a shows the Mon block, brick block and LW block specimens, whereas Fig. 1a shows the composite infill walls and SIP walls. The plaster in specimens w1-p, w2-p and w3-p was 8mm thick, as shown in Fig. 1c. Fig. 1d shows all the specimens before testing. Table 1 summarises the physical and thermal properties of the wall systems examined in Phase 1. The last three columns of the table also include the thermal properties of the materials used to build the new UWall SIP, as described later in section 2.2.1.

**Table 1**. Physical and thermal properties of wall systems tested in Phase 1

| **Properties** | **Conventional materials** | | | **EPS SIP** | | **PU SIP** | | **Infill wall** | | **UWall SIP** | | |
|---|---|---|---|---|---|---|---|---|---|---|---|---|
| | Mon block | Brick block | LW block | Cement board | EPS foam | Cement board | PU foam | Cement board | Foamed concrete [a] | Cement board | EPS foam | Foamed concrete [a] |
| Density (kg/m$^3$) | 1640 | 1600 | 1170 | 1300 | 1000 | 1300 | 961 | 1300 | 3600 | 1300 | 1000 | 3600 |
| Thermal conductivity (W/m×k) | 0.69 | 0.7 | 0.29 | 0.93 | 0.036 | 0.93 | 0.028 | 0.93 | 0.075 | 0.93 | 0.036 | 0.075 |
| Specific heat (J/kg×k) | 800 | 840 | 1000 | 920 | 1100 | 920 | 1100 | 920 | 1000 | 920 | 1100 | 1000 |
| Thermal transmittance W/(m$^2$×K) [33] | 2 | 1.75 | 1.23 | 0.37 | | 0.22 | | 0.15 | | | | |

Note: [a] Foam concrete made of Expanded Polystyrene (EPS) beads mixed with cement mortar (OPC Type I and fine recycled concrete aggregate).


(a)

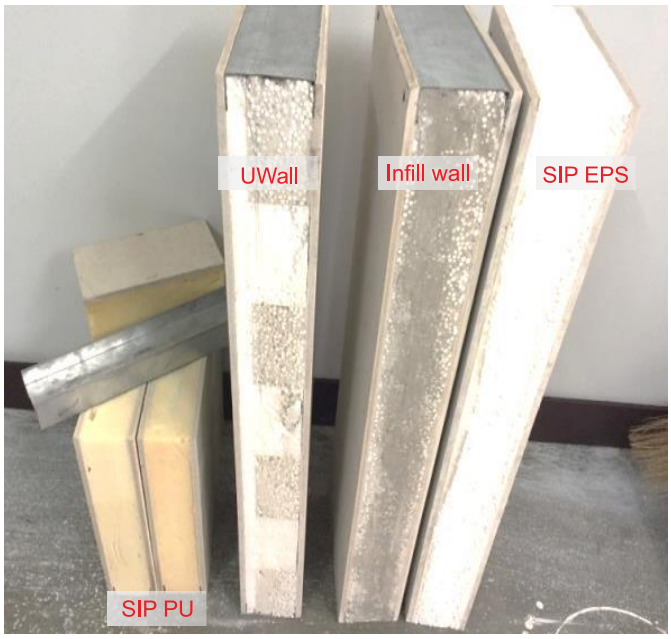


(b)

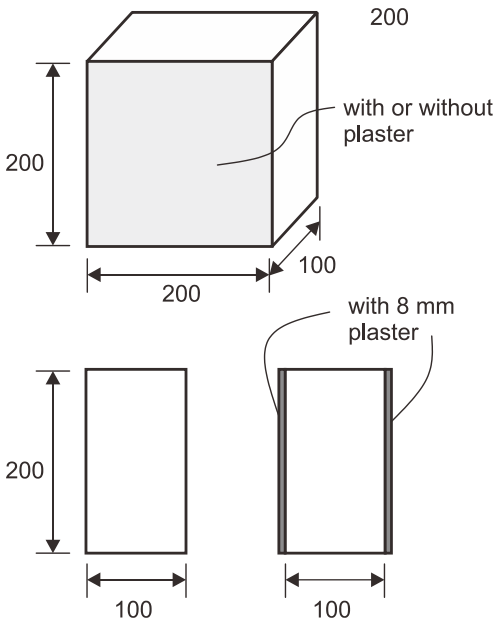


(c)

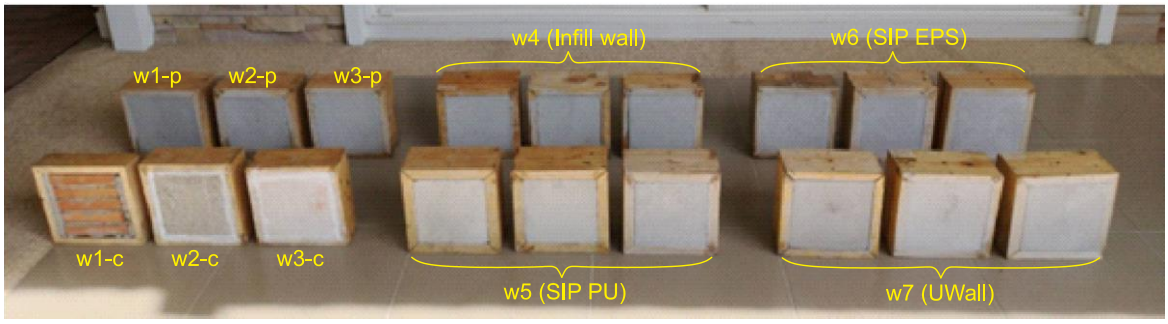


(d)

**Fig. 1**. Specimens tested in Phase 1: (a) conventional wall materials, (b) SIPs and infill walls, (c) specimen geometry (units: mm), and (d) specimens before tests.

The specimens were placed inside an ad-hoc thermal chamber, as shown in Fig. 2a. Heat was supplied continuously on the inner face of the specimens until its outer surface temperature reached 70°C (the maximum temperature of the chamber), after which the source of heat was switched off. The temperature and RH were measured using Resistance Temperature Detector (RTD with DIN Class A)

sensors (Fig. 2b) and recorded for 12 hrs for both heating up and cooling down stages at locations RTD1 to RTD4 (Fig. 2a). Note that sensor RTD1 was placed on the specimens' face with 300 mm away from the heat source, whereas RTD3 was on the opposite face of the specimens. The heat source produced by a 250-watt heat lamp induced temperature of 70 $^{o}$C and maintained during the test using a temperature control. Based on the results from these initial tests, five wall systems were selected to build the house units and full-scale house tested in Phases 2 and 3, as explained in subsequent sections.

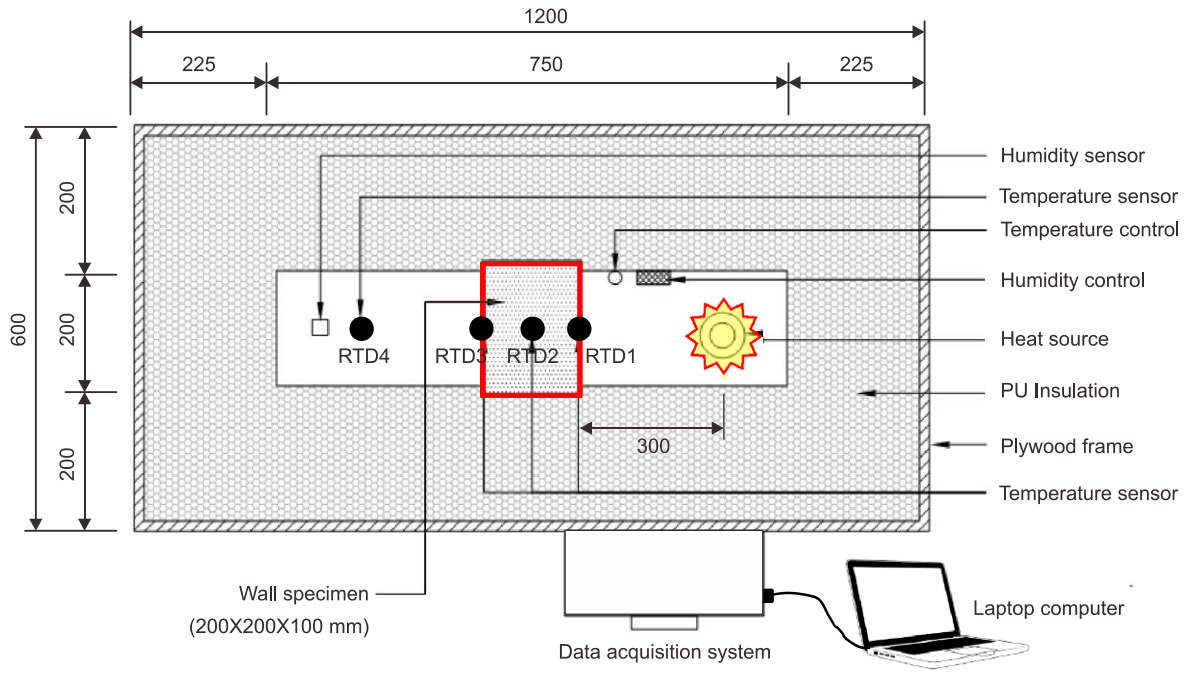


(a)


(b)

(c)

**Fig. 2**. Tests in Phase 1 (a) schematic view of test setup and instrumentation (units: mm), (b) view of ad-hoc chamber and (c) Resistance Temperature Detector (RTD with DIN Class A).

## 2.2. Phase 2: Structural tests on UWall SIPs and scaled-down housing units

### *2.2.1. Construction of UWall SIP panels*

***i)*** ***Geometry and construction.*** The core material of UWall SIPs consisted of an EPS waffle panel and lightweight foamed concrete, both packed within two cement boards (see schematic view in **Fig. 3**a). The UWall SIPs had a size of 600×2800 mm and were designed according to typical heights of houses in Thailand [6, 34, 35]. The total thickness of the new panel (100 mm, see **Fig. 3**b) replicates typical thicknesses of walls used in Southeast Asian construction practice. Fig. 3c shows the waffle EPS skeleton used for the SIP, whereas Fig. 3d shows the filling of the waffle gaps with foamed concrete and a slump of 50 mm.

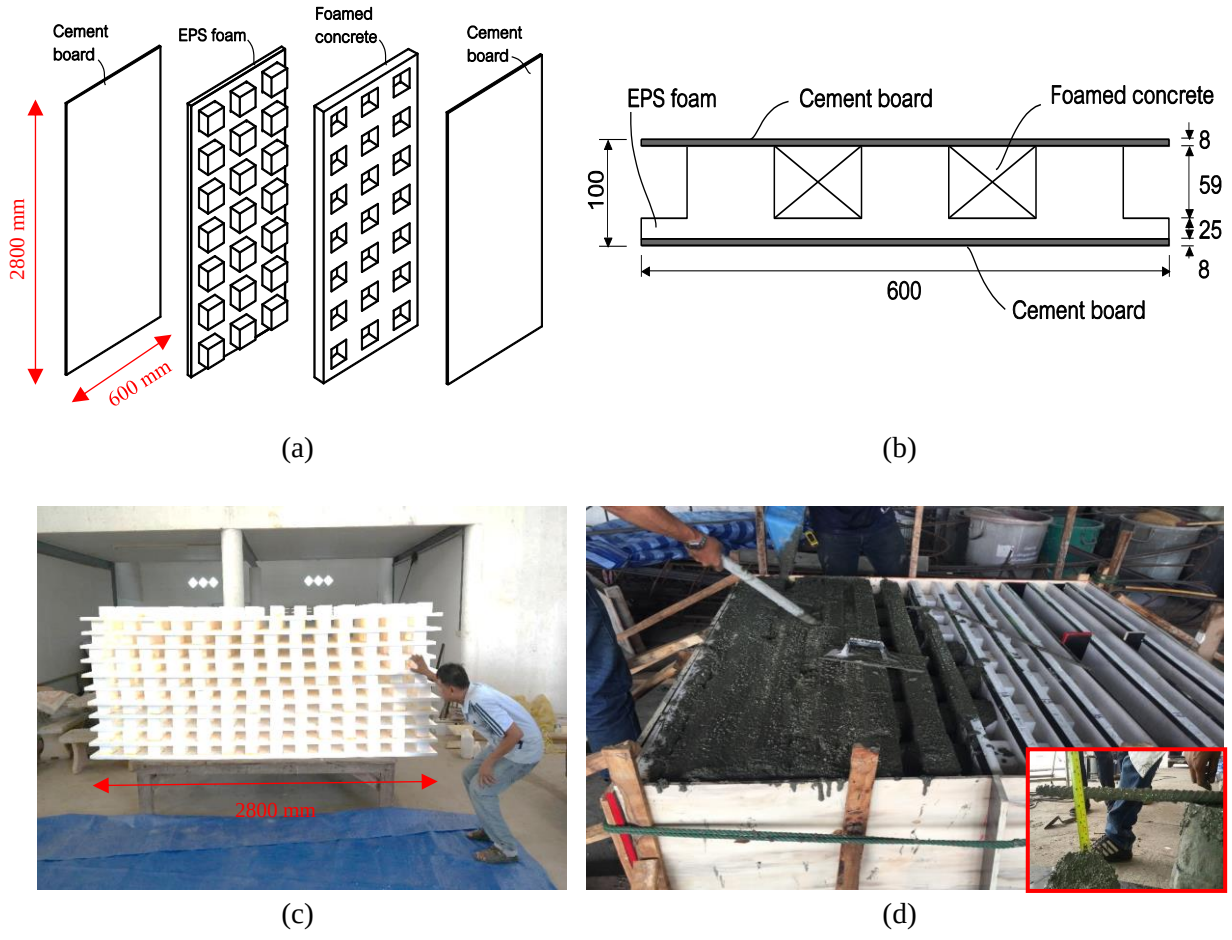


(a) (b)

(c) (d)

**Fig. 3**. UWall SIP: (a) geometry and components, (b) cross section (in mm), (c) waffle EPS, and (d) laying of foamed concrete.

***ii) Foamed concrete.*** The foamed concrete of the UWall SIPs was made of ordinary Portland cement (OPC) Type I and recycled concrete aggregate (RCA). The RCA was recoverd from old concrete cylinders crushed with an an ad-hoc crushing machine. Fine recycled concrete aggregate (RCA-FA) was

crushed from coarse aggregate (RCA#1) and used in the fomead concrete mix design, as shown in **Fig. 4**a. The physical and mechanical properties of the RCA are summarised in **Table 2**. The mix design (per 1 $m^3$) of the foamed concrete was: 50 kg of OPC Type I, 25 kg of RCA-FA, 25 l of water, 1.4 kg of EPS beads (3-5 mm diameter with density of 1.25 $lb/ft^3$), and 15 g of a foam dispersive agent (**Fig. 4**b). The target slump was 50mm. Six 100mm cubes and six 100×200mm cylinders were crushed to strength of the foamed concrete. Table 3 summarises the mechanical properties of EPS, cement board and foamed concrete.


(a) (b)

**Fig. 4.** (a) Recycled concrete aggregate (RCA) used in foamed concrete, and (b) EPS beads and foam dispersive agent.

**Table 2.** Physical and mechanical properties of recycled concrete aggregates.

| **Properties** | **Recycled concrete aggregates** | |
|---|---|---|
| | **Coarse RCA#1** | **Fine RCA-FA** |
| Bulk specific gravity (SSD) | 2.51 | 2.77 |
| Unit weight ($kg/m^3$) | 1425 | 1400 |
| Water absorption (%) | 5.13 | 2.65 |
| Moisture (%) | 2.14 | 2.42 |
| Fineness modulus | - | 1.8 |
| Max. size (mm) | 9.8 | 4.70 |
| Impact value (%) | 12.5 | - |
| Crushing value (%) | 20.12 | - |
| Residual mortar (%) | 30.2 | 32.5 |

**Table 3.** Mechanical properties of UWall SIPs components.

| **Materials** | **Compressive strength (MPa)** | **Modulus of elasticity (MPa)** | **Poisson's ratio** |
|---|---|---|---|
| Cement board[a] | > 20 | > 4500 | 0.2 |
| EPS (1.25 $lb/ft^3$)[b] | 0.10 | 2.00 | 0.08 |
| Foamed concrete[b] | 9.06 (12.3) | 14240 (15012) | 0.18 (0.19) |

[a] Provided by manufacturer [5, 6], [b] Obtained from laboratory test for cylinder followed by the results from cube specimens in parentheses.

### *2.2.2. Structural panel tests*

Structural tests were carried out to establish the capacity of the UWall SIPs. Two SIP configurations were considered: a) SIPs "A" made of an EPS core and foamed concrete, and b) SIP Type B which was similar to SIP Type A but it had a cold-form steel channel (C75x45x3 mm) so as to replicate the way the panels are installed and connected in actual houses. Two specimens (A-1, B-1) with the same loading arrangement, were subjected to pure axial load (load P1) to investigate their maximum axial capacity ($P_{max}$), as shown in **Fig. 5**a. The rest of the specimens (A-2 to A-8, and B-2 to B-8) were subjected to combined axial load (load P1 as a fraction of $P_{max}$) and four-point bending (loads P2). The SIP specimens had a rectangular cross-section of 100×600 mm and a free span length of 2400 mm (**Fig. 5**a). Vertical deflections were measured using Linear Variable Displacement Transducers (LVDTs) with an accuracy of 0.001 mm. **Table 4** presents the details of the UWall SIPs tested in Phase 2. The results from these tests were used to derive design charts for the design of the full-scale house described later in Phase 3.

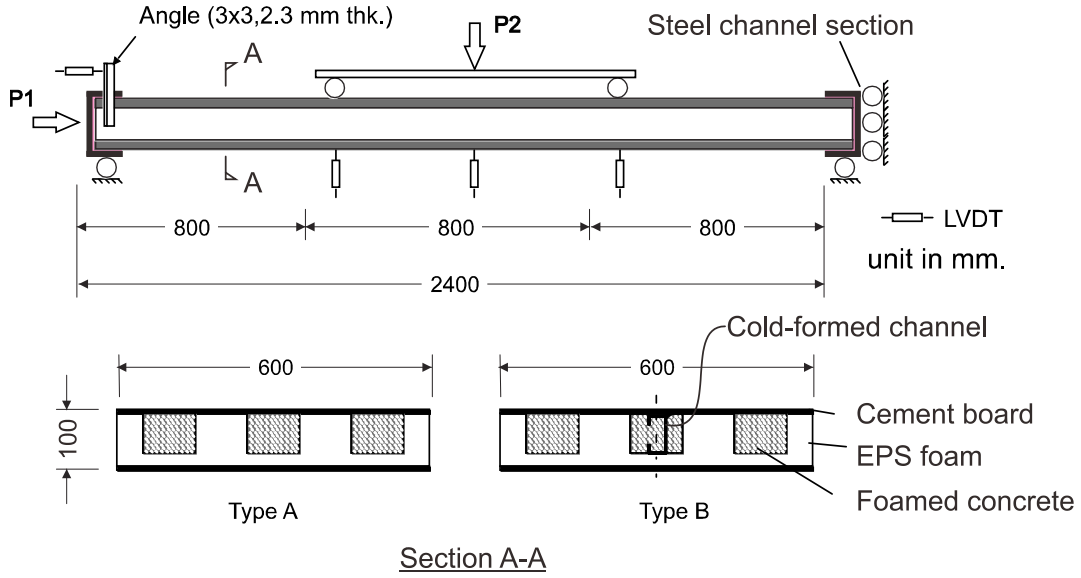


(a)

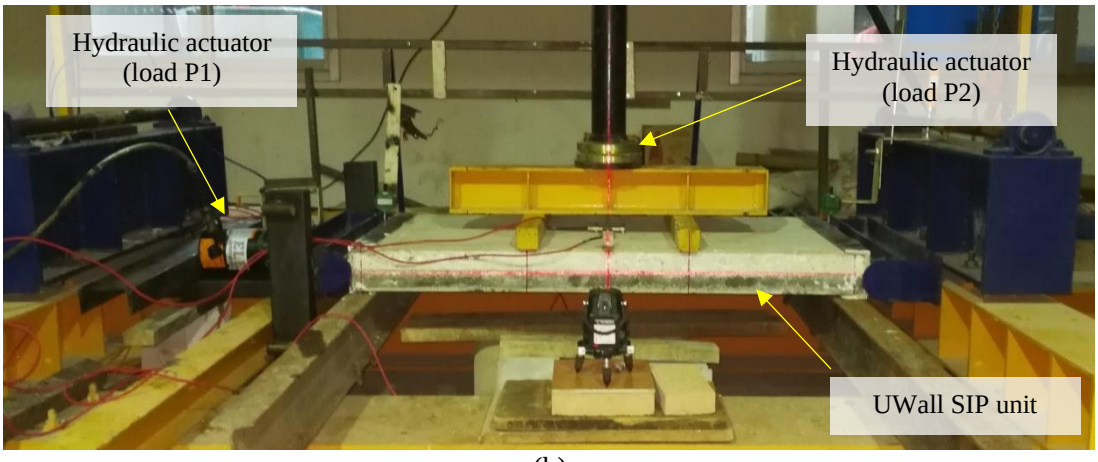


(b)

**Fig. 5**. Structural tests on UWall SIPs in Phase 2: (a) schematic setup and geometry, and (b) view of a typical panel during testing.

**Table 4.** Details of structural tests on UWall SIPs under combined axial and bending.

| Panel ID | Axial load (P1) | Bending load (P2) |
|---|---|---|
| A-1, B-1 | $P_{max}$ | - |
| A-2, B-2 | $0.10P_{max}$ | Increasing up to failure |
| A-3, B-3 | $0.15P_{max}$ | Increasing up to failure |
| A-4, B-4 | $0.25P_{max}$ | Increasing up to failure |
| A-5, B-5 | $0.50P_{max}$ | Increasing up to failure |
| A-6, B-6 | $0.75P_{max}$ | Increasing up to failure |
| A-7, B-7 | $0.90P_{max}$ | Increasing up to failure |
| A-8, B-8 | - | Increasing up to failure |

### *2.2.3. Scaled-down house units*

Fig. 6 shows the locations of a full-scale house and seven scale-down houses together with the sun path in north hemisphere. To assess the thermal performance of different wall systems under more realistic conditions, five scale-down house units (see Fig 7.a-g) were built in Chachoengsao province, Thailand. The scaled-down house units consisted of a base of 1.5×1.5 m, and a headroom of 2.4 m. The walls of the seven scaled-down houses were built with the following materials: a) H1 with Mon blocks w1-c (Fig 7.a), b) H2 with brick blocks w2-c (Fig 7.b), c) H3 built with LW blocks w3-c (Fig 7.c), d) H4 built with composite infill walls w4 (Fig 7.d), e) H5 built with SIP PU walls w5 (Fig 7.e), f) H6 built with SIP EPS walls w6 (Fig 7.f), g) H7 with U-Wall panels w7 (Fig 7.g). The house units were mounted on wheels and therefore the floor was raised 0.15 m above the ground. The house units were fitted with a PVC door (0.7 m wide×1.8 m high) and a glass window (0.5 m wide×0.8 m high).

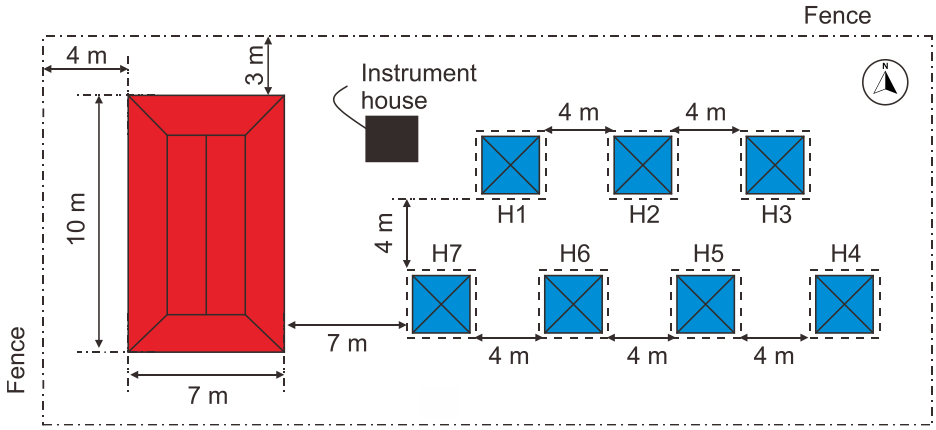


**Fig. 6.** Locations of a full-scale house (U-Wall SIP) and scale-down houses (H1 – H7).


**Fig 7**. Full-scale house by Hybrid wall panel and Scaled-down house units built with: (a) Mon blocks (H1), (b) brick blocks (H2), (c) LW blocks (H3), (d) composite infill wall panel (H4), (e) SIP PU (H5), (f) SIP EPS (H6), and (g) UWall panel (H7).

Fig 8. shows the locations of temperature (outdoor $T_o$ and indoor $T_i$) and RH measuring points. The temperature was measured for one week and recorded every 30 min using a high precision temperature detector with an accuracy of ±0.01°C (RTD sensor), with a range of -50.0°C to 330.0°C. Temperatures were measured in mid-March, which is the hottest month in Thailand. Two Scenarios were considered: Scenario 1) with indoor air movement (i.e., both door and window opened), and Scenario 2) without indoor air movement (i.e., door and window closed). Ground-level air speed (ranged 1-1.5 m/s) was also monitored at 3 m above the ground.

From the energy saving measurement, it is a study comparing the rate of energy loss in the amount of electrical units of mobile air conditioners for a period of 7 days between –at the hottest month in Thailand (22-30 April 2019) by measuring the electrical units from the power meter as shown in Fig 8c. Performance of wall material will also be assessed by mean of electrical unit consumption by turning on the mobile air conditioner for 24 hours a day for 30 days.

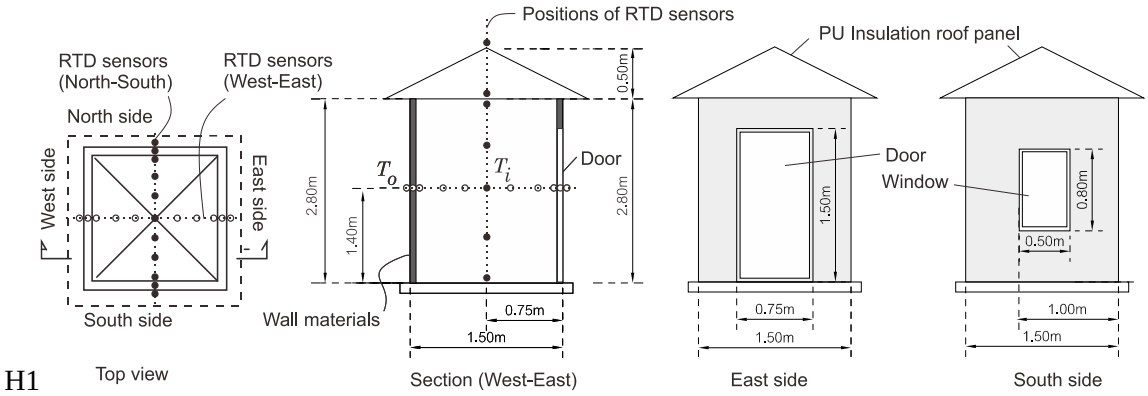


(a)

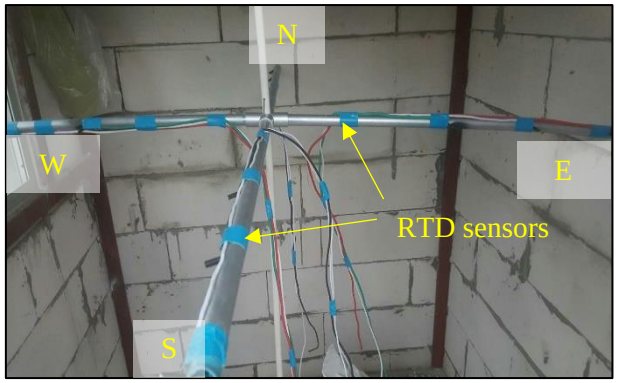


(b)


(c)

**Fig 8**. Measuring points showing outer and inner RTD sensors in scaled-down housing units in Phase 2 (a), inside view of RTD sensors (b) and electric unit meter used to measure energy consumption of AC in scaled-down H2 (c).

### 2.3. Phase 3: Full-scale house

A house of 10×7 m in plan was built with UWall panels in Chachoengsao province, Thailand. The floor was elevated 0.6 m from the ground according to local construction practices. All the 2.8 m-high walls were build using the new UWall SIP developed in this study. No beams or columns were provided to the house. The house was designed using local regulations for dead loads and live loads. Accordingly, the design floor live load was 1.5 kN/m$^2$ (a typical value for housing in Thailand), while the roof live load was 0.3 kN/m$^2$. The wind load (5 kN/m$^2$ for a building height less than 10 m) was also considered in the design. The above loads led to the dimensions shown previously in Fig. 3b.

First, the concrete floor was cast. A ready mixed concrete with a strength of 24 MPa was used for casting the precast slabs (thickness of 50 mm) combined with 6 mm welded wire reinforcing mesh ($F_y$= 235 MPa, $E_s$ =200 GPa) to achieve an overall slab thickness of 100 mm. Next, the piping and electric works and U-Wall SIPs were installed (Fig. 9a). The UWall SIPs were connected to each other using vertical cold-form steel channels (C75×45×3 mm) placed at 600 mm centres. The channels were then fixed to the concrete floor using brackets. Doors and windows were fixed after the installation of the SIPs. The house was carefully designed to optimise the material and labour cost. Supplementary Data gives an overview an indoor and outdoor tour of the full-scale house taken on 14 April 2023 in Appendix D.

(a)

(b)


(c)

**Fig. 9**. Construction of a full-scale house with UWall panels; (a) installation of UWall SIPs and (b) overview of full-scale house and instrument house.

**Fig. 10** shows a plan view of the full-scale house and the location of RTD sensors. Sensor RTD1 measured the outdoor temperature, whereas sensors RTD2 and RTD3 measured the indoor temperatures in the rooms. All sensors were located at the mid-height (1.4 m) of the walls. The RH was measured using a digital hygrometer HTC-2 (RH range=10-99%). The outdoor wind speed was measured with an AS816 air velocity meter (measuring range=0.3-2.0 m/s) at 3.0 m above the ground for 48 hrs. Likewise, field data in terms of indoor temperature, RH and air movement were recorded twice during four measuring periods: 07:00 -10:00 hrs, 11:00 -17:00 hrs, 18:00 -22:00 hrs, and 23:00-06:00 hrs.

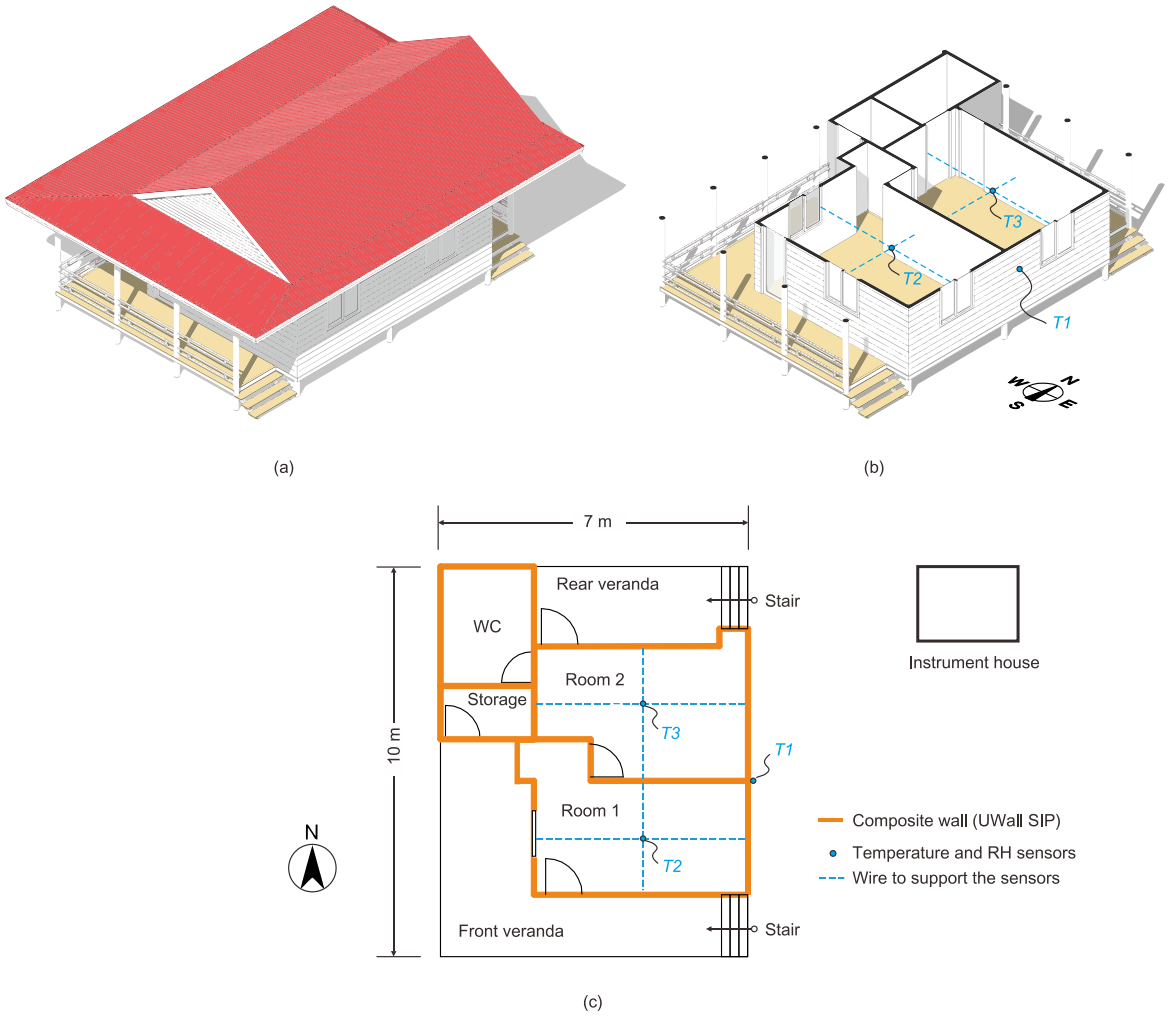


**Fig. 10**. Filed measuring of the full-scale house: (a) Outside view of the house, (b) inside view of the house showing monitored rooms with sensors (T2, T3) located inside and outside (T1) the full-scale house (c).

## 3. Results and discussion

### 3.1. Phase 1: small specimens

Fig. A-1 in Appendix A shows the temperatures measured by sensors RTD1 to RTD4 during the test. Table 5 compares the temperatures measured on the specimens, as well as it's normalized value from 70$^{o}$C (shown between brackets). The temperatures measured by RTD3 show that the UWall specimen outperforms other specimens in terms of thermal performance. Specifically, it performs 20%, 12%, 10%, 12.4%, 7.6%, and 9.2% Lower temperature than w1-c, w2-c, w3-c, w1-p, w2-p, and w3-p specimens, respectively. Moreover, the UWall SIP also records lower temperatures compared to the infill wall, PU SIP, and EPS SIP by up to 7.6%, 3.8%, and 2%, respectively. It should be noted that the wall systems marked with an asterisk in Table 5 (column ID) were selected to build the scaled-down house units in Phase 2. The selected wall systems are extensively used in the construction of houses in Southeast Asia.

**Table 5.** Test results from Phase 1: temperature distribution along the walls from the source temperature of 70°C acting on the front side of the specimens.

| ID | Type of material | Type of plastering | Measured temperatures (°C) | | | |
|---|---|---|---|---|---|---|
| | | | RTD 1 | RTD 2 | RTD 3 | RTD 4 |
| w1-c * | Mon block | Control (no plastering) | 70 (100%) | 38.2(-54.6%) | 32.7(-46.7%) | 30.0(-42.9%) |
| w2-c * | brick block | | | 37.4(-53.4%) | 31.2(-44.6%) | 28.0(-40.0%) |
| w3-c * | LW block | | | 34.3(-49.0%) | 30.2(-43.1%) | 27.5(-39.3%) |
| w1-p | Mon block | Plastered with mortar | | 37.2(-53.1%) | 30.1(-43.0%) | 26.9(-38.4%) |
| w2-p | brick block | | | 35.2(-50.3%) | 30.4(-43.4%) | 27.3(-39.0%) |
| w3-p | LW block | | | 32.8(-46.9%) | 28.7(-41.0%) | 26.6(-38.0%) |
| w4 * | Infill wall | No plastering | | 33.6(-48.0%) | 28.0(-40.0%) | 25.5(-36.4%) |
| w5 | PU SIP | | | 28.5(-40.7%) | 27.0(-38.6%) | 25.2(-36.0%) |
| w6 | EPS SIP | | | 27.5(-39.3%) | 26.5(-37.9%) | 25.1(-35.9%) |
| w7 * | UWall SIP | | | 28.0(-40.0%) | 26.0(-37.1%) | 25.0(-35.7%) |

**Note:** * Walls selected to build scaled-down house units in Phase 2.

### 3.2. Phase 2: structural tests and scale-down house units

#### *3.2.1. Structural tests*

Fig. 11a shows the bending load (P2) vs mid-span deflection results of the tested UWall SIPs. The results in Fig. 11a indicate that the bending behaviour of the walls was essentially linear up to failure. SIPs "B" (with a C- cold-form section) exhibited a consistently higher bending capacity compared to SIPs "A". It is also shown that the bending capacity of the UWall SIPs reduced as the axial load increased above 0.50-0.75$P_{max}$. UWall SIPs A-7 and B-7 had the highest axial load (0.9$P_{max}$) and this resulted in premature failures at relatively low mid-span deflections of about 13-17 mm. In general, SIPs "B" had lower deflections at ultimate failure but higher bending capacity. Despite this, the data in Fig. 11a confirm that all the tested SIPs "A" and "B" met the deflection limits (Span/333 = 7.20 mm) specified by Eurocode 6 [36]. The ultimate failure mode of the SIPs was dominated by rupture at the mid-span region, as shown in Fig. 11b.

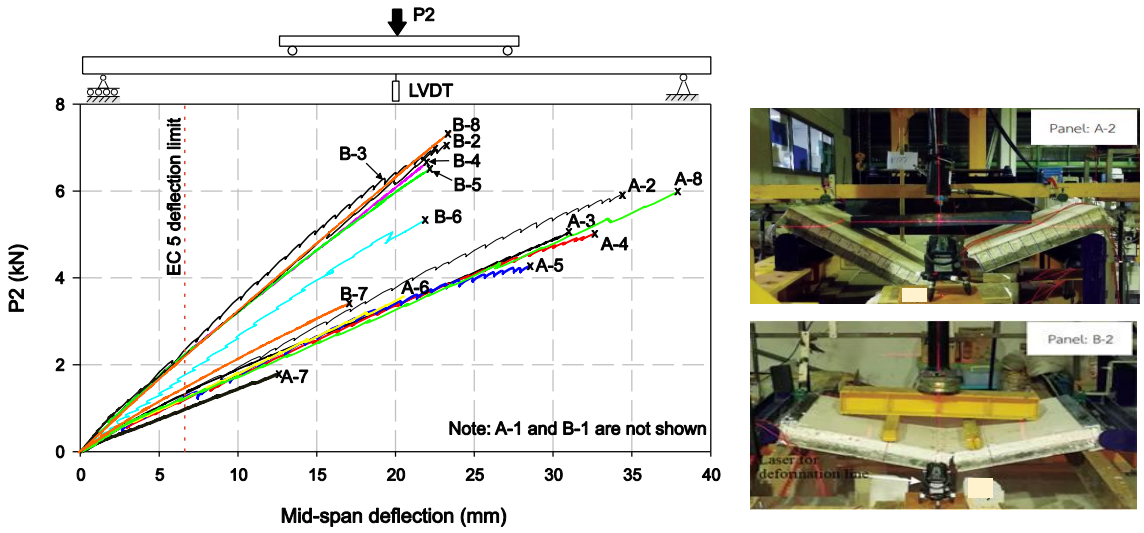


(a) (b)

**Fig. 11.** Structural test results from Phase 2: (a) bending load vs mid-span deflection curves of UWall SIPs, and (b) typical failure modes.

Based on the test results, initial design charts for the novel UWall SIPs are proposed here. Fig. 12 shows P-M interaction diagrams per metre width of SIPs "A" and "B", which were obtained using a least square method and a cubic polynomial equation. The design charts can be constructed with the different values of reduction factor ($\phi$). Accordingly, a power reduction factor $\phi$=0.50 is proposed for the sample wall exhibiting a linear elastic behaviour (see Fig. 12a). For example, with safety margin factor $\phi$ =50%, any load combinations obtained from the structural analysis of the panels (P-M) should lie within the red dotted line. For the structural analysis, since the wall panels were designed as a load-bearing panel to resist both vertical and horizontal loads, a computer programme was used to create a 3D finite element model as shown in Fig. 12b. The load combinations used in the analysis consisted of

1) self-weight; 2) service load (DL+LL) and 3) factored load (1.4DL+1.7LL). The maximum moment in longitudinal direction ($M_x$) developed in the wall panels was about 440 kg-m per meter (4.31 kN-m / meter) and the axial compression ($P_y$) force induced in the wall panel was about 1530 kg per meter (15 kN / meter). **Fig. 12** shows the P-M interaction diagram of the UWall panel with the analysis results. As seen in the figure, the combination of the maximum factored moment and factored axial forces were computed and found to be within the P-M design chart ($\phi$=50%) and therefore, the wall panels can be successfully used as a load bearing panel for the house. it is also proposed that the reduction factor, $\phi$=50% should be used as a design chart for the UWall panels (**Fig. 12**b).

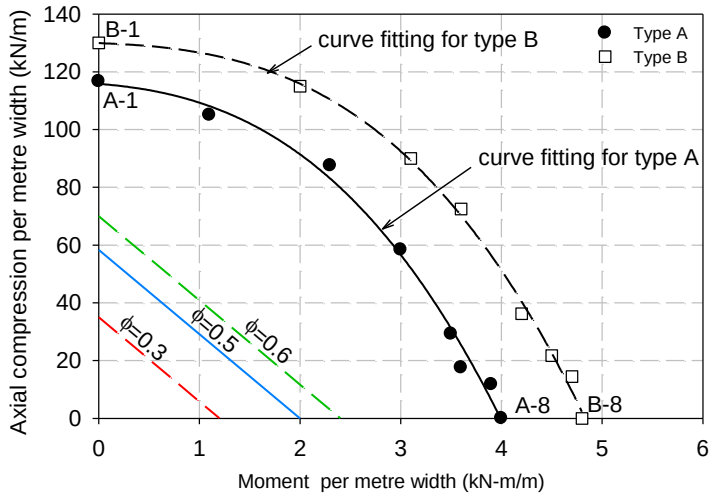


(a)

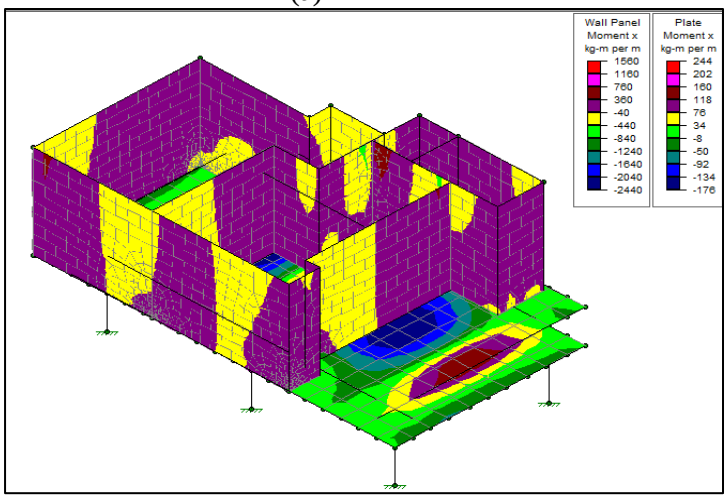


(b)

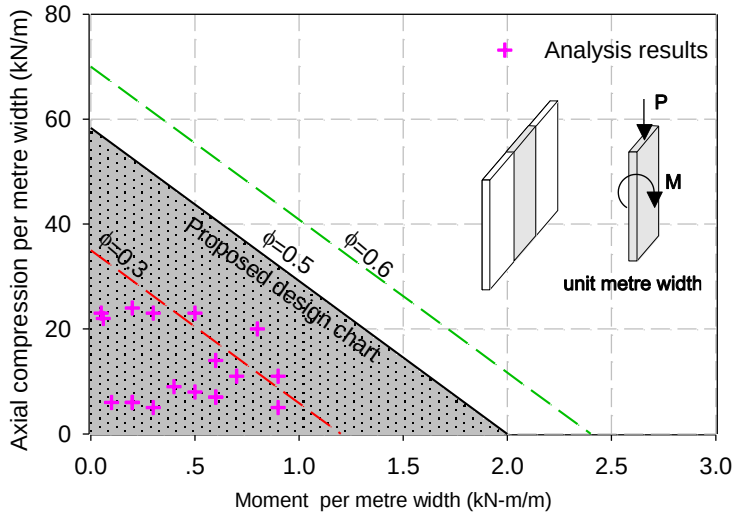


(c)

**Fig. 12.** Development of design diagram of UWall SIPs; (a) P-M interaction diagram with analysis results, (b) Structural analysis of full-scale UWall SIP house and (c) P-M interaction diagram with analysis results.

### *3.2.2. Thermal performance*

Fig. 13a compares the temperature and RH recorded in the seven scale-down house units H1 to H7. The data correspond to indoor sensor $T_i$ (located at 1.4 m above the unit floor) compared to the outdoor temperature and RH at point $T_o$. Results for both Scenario 1 (air movement) and Scenario 2 (no air movement) are reported. The results in Fig. 13a show that, in the case of Scenario 1 (grey-shaded region), the air temperature in the UWall unit H7 is consistently 3° to 5°C lower than in the other four house units. Fig. 13b shows that, in the case of Scenario 2, the RH of the air outside and the humidity of the air inside the seven house units were similar and close to 70-80% between 0:00-7:00 hrs. However, at 08:00 hrs, the relative humidity (RH) decreased due to a minimal temperature difference between the indoor and outdoor environments. The RH gradually increased after 13:00 hrs because of the temperature variation indoors varies with the movement of sun and the heat penetration through the opening of door and windows. Fig. 13b also shows that, in the case of Scenario 1 (i.e., door and window opened), the outdoor RH (ambient) of the building at 15:00 hrs was 90%. The indoor RH was high due to the lower indoor temperature, which caused less moisture to vaporise inside the room. The ambient RH was relatively high (90-93%) between 21:00 to 03:00 hrs due to shower rain. During the daytime, from 0:00 to 07:00, it was observed that the relative humidity of the outdoor air and the indoor air of all 7 sample houses had similar values, ranging from approximately 70% to 80%. The humidity then gradually decreased at 08:00 and started to increase around 13:00. The measurements of relative humidity showed a consistent pattern of fluctuations over a 48-hour period.

The influence of Scenario 1 (i.e., door and window opened) on the indoor relative humidity of the simulated houses is illustrated in Fig.14b. The indoor relative humidity was found to decrease when the doors were closed. This is because the indoor humidity of the simulated houses can be effectively dissipated to the outside through the open spaces. When considering the trend of indoor humidity in the simulated houses constructed with composite compressed earth block walls, it was found to remain relatively stable, except during rainfall events, and when there were open spaces available.

The results in this section confirm that the indoor RH in H7 was 15% less for a given outdoor temperature because less moisture is vaporised by the UWall due to heat absorption.

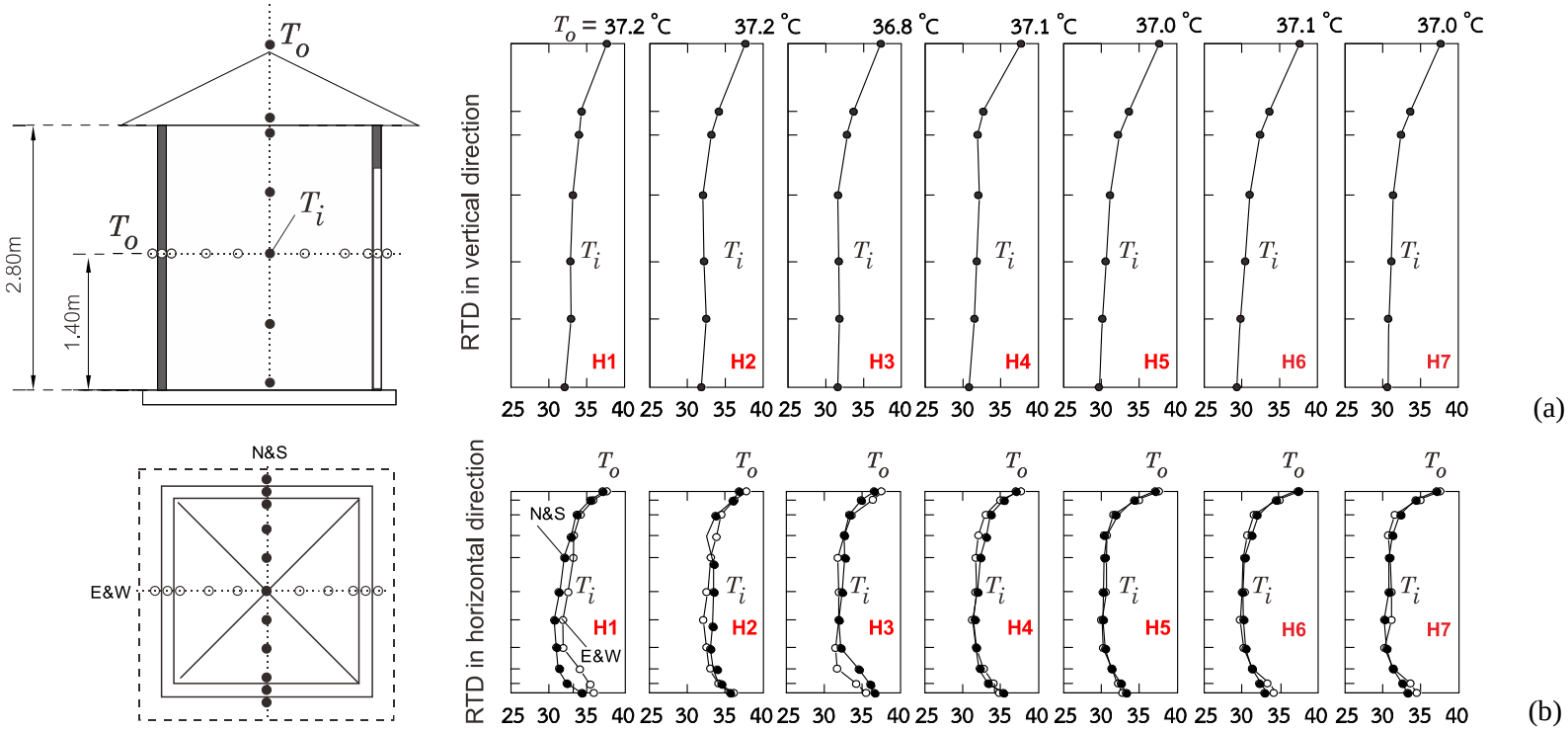


**Fig. 13**. Scale-down house units: (a) indoor temperatures and (b) RH measured for different Scenarios at point $T_i$ compared to outdoor (ambient) temperature and RH at point $T_o$.

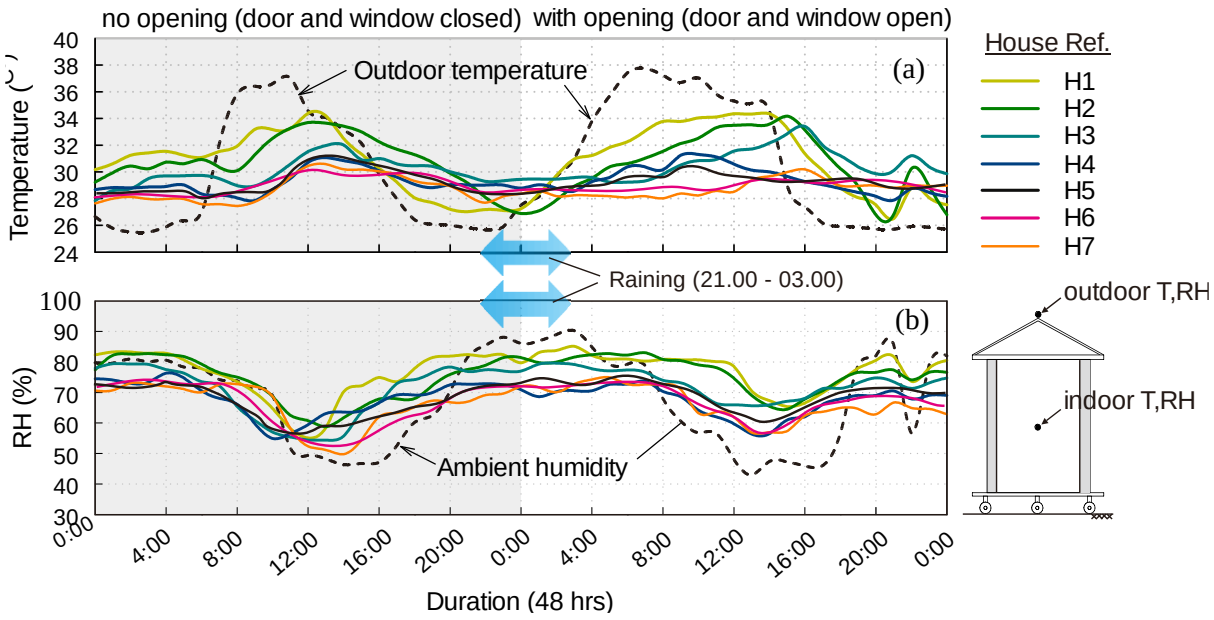


**Fig. 14**. Scale-down house units: (a) indoor temperatures and (b) RH measured for different Scenarios at point $T_i$ compared to outdoor (ambient) temperature and RH at point $T_o$.

### *3.2.3. Energy consumption*

Study of the energy efficiency of walls in the form of energy-saving walls with installed portable air conditioners inside a simulated house for a period of 30 days, from 1-30 April 2019, by measuring the amount of electricity from the electricity meter shown in Fig. 15. It was found that the amount of electricity consumed by a 6000 BTU air conditioner running continuously for 24 hours over a period of 30 days is lowest in the simulated house H6, which was constructed using Structural Insulated Panels (SIP) with Expanded Polystyrene (EPS) as the core material. The order of electricity consumption, from lowest to highest, is as follows: H6, H7, H3, H4, H5, H2, H1, respectively. It can be observed that SIP walls with cored material made of Polyurethane (PU) as the core material do not exhibit high electricity consumption compared to other conventional wall materials. Additionally, the Infill wall (H4) has electricity consumption similar to that of the LW wall (H3), while the electricity consumption of H1 is the highest. Fig. 15b provides a comparison of electricity consumption per unit over the 30-day period, in the following order: H1 (100%), H2 (98%), H3 (85%), H4 (91%), H5 (92%), H6 (62%), H7 (74%).

The results obtained from the measurements in Fig. 15a can be used to create a regression line by considering the best-fitting equation based on the $R^2$ value. For the simulated SIP UWall (H6), the linear regression equation is found to be $E_n = 45.90x\text{-}59$, where $E_n$ represents the electricity consumption and x represents the duration of time considered (in days). Therefore, we can predict the electricity consumption for a period of 30 days for each simulated house based on the field data, assuming an electricity cost of 5 Baht per unit (without considering variable rates and deductions that equals to about 0.12 pounds). The predicted electricity consumption is shown in Fig. 15c. When examining the proportion of the increase in electricity consumption for air conditioners running continuously for 24

hours for each type of simulated house wall, noticeable changes can be observed after three years. Walls constructed with Mon bricks and concrete blocks have the highest electricity consumption. On the other hand, SIP EPS foam as the core material have the lowest electricity consumption, followed by SIP UWall, followed by LW brick and infill wall, respectively.

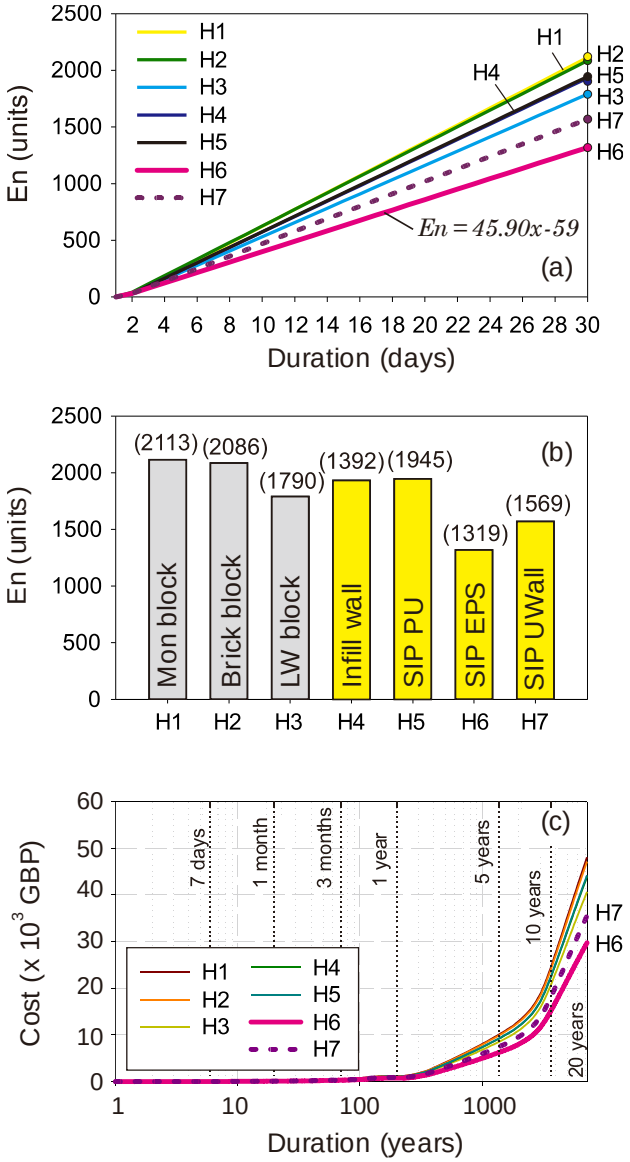


**Fig. 15**. Comparison of energy consumption measured for 30 days for scale-down houses (a), total unit usages of different wall materials (b) and forecast of the energy consumption over 20 years (c).

Based on the findings from experimental work carried out in phases 1 and 2, the novel finding of this study revealed that the simulated house with composite compressed earth block walls, utilizing EPS foam as the core material, exhibited the highest performance in heat and moisture insulation, resulting in the most effective protection against heat transfer and moisture infiltration. Additionally, it demonstrated the lowest energy consumption rate. In contrast, the traditional Mon brick wall,

representing the conventional construction method, was found to have the highest energy consumption rate. Nevertheless, SIP Wall exhibits great both thermal resistance and structural load bearing wall [37, 38].

The following section discusses the results from the full-scale house built with UWall SIPs using temperature absorption and RH.

### 3.3. Phase 3: full-scale house

Fig. 16a-b show the recorded temperature and RH of the full-scale house for Scenario 1 (air movement) and Scenario 2 (no air movement). The results show that, for Scenario 2 (Fig. 16a), the indoor temperatures measured by sensors T2-T3 were lower than those recorded by T1. This is attributed to the fact that moisture present inside the house cannot be released into the air and can only exchange energy with its surroundings. However, between 20:00 to 24:00 hrs, the indoor temperatures recorded by T2 and T3 were higher than the outdoor temperature T1 because the heat stored in the wall during the day was released at night-time.

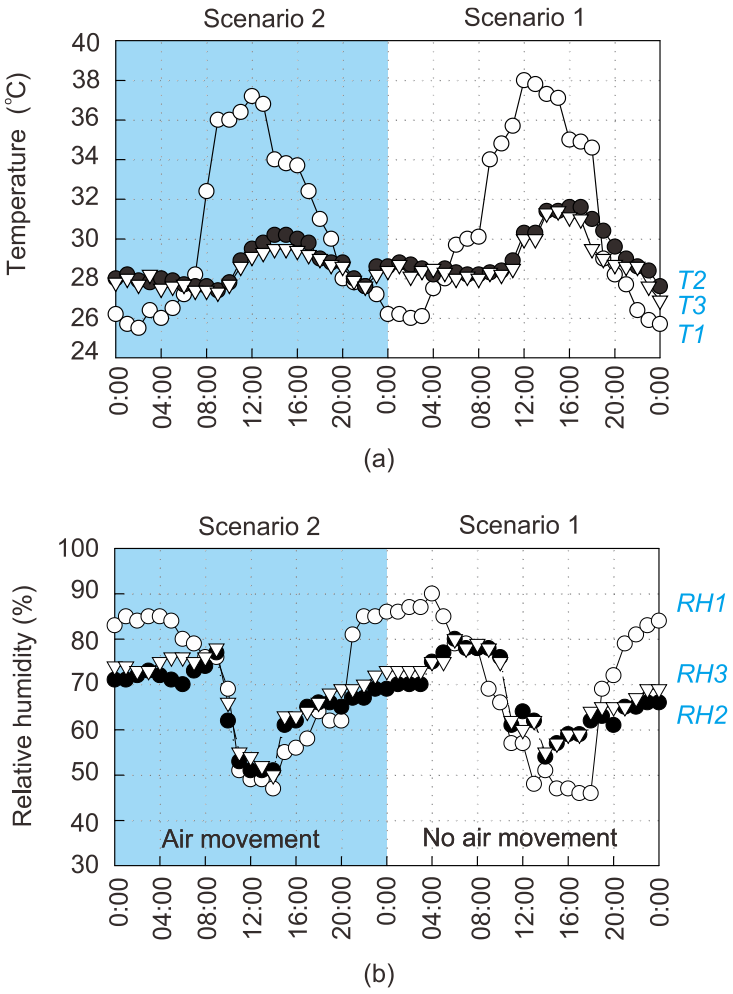


**Fig. 16.** Full-scale house: (a) temperatures, and (b) RH recorded for 48 hrs for different Scenarios.

Based on 48 hrs of monitoring, the results in Fig. 16a show that the highest outdoor temperature was 37°C between 12:00–13:00 hrs, whereas the highest indoor temperature was 31°C between 12:00–16:00 hrs. Accordingly, the difference between indoor and outdoor temperatures was about 5°C and 7°C for Scenario 1 and Scenario 2, respectively. At night-time (21:00-05.00 hrs), the outdoor temperatures T1 were about 2°C and 3°C higher than the indoor temperatures at T2 and T3 for Scenario 1 and 2 respectively. This can be attributed to the UWall SIPs releasing heat absorbed during daytime.

The results in Fig. 16b show that the ambient RH was very high (90%) at 04:00 hrs, since it rained around that time for Scenario 1. However, the indoor RH at $RH_2$ and $RH_3$ was lower than the outdoor $RH_1$ by up to 15%.

In the field of building design, Givoni [5] introduced bioclimatic charts that serve as a valuable tool. These charts take into consideration several factors such as air temperature, humidity, mean radiant heat, air movement, solar radiation, and cooling through evaporation. By analyzing these variables, the charts establish a comfort zone within which occupants can experience optimal comfort. The defined comfort zone typically ranges between 21.0°C and 27.5°C. However, it is worth noting that this range can slightly shift downward during winter or upward during summer, accommodating seasonal variations. For instance, in the case of Chachoengsao province, the meteorological data provided in Appendix B reveals that the mean daily minimum air temperature ($T_{m,min}$) in December is 15.2°C. On the other hand, the mean daily maximum temperature ($T_{m,max}$) in August reaches 33.3°C. These figures help to contextualize the local climate conditions and aid in designing buildings that offer optimal comfort to occupants throughout the year. By incorporating bioclimatic charts and analyzing the specific climatic data for a given location, architects and designers can make informed decisions to create sustainable and comfortable living and working environments.

**Fig. 17**a-b show bioclimatic charts (temperature vs RH) of the full-scale house for Scenario 1 (air movement) and Scenario 2 (no air movement). The data for Scenario 1 (Fig. 17a) show that the temperatures and RH in the house were slightly outside the comfort zone. In the case of Scenario 2 the average air movement was also recorded and found to be about 0.4 m/s with windows/doors open.

Therefore, it is concluded that the house model constructed using UWall lied within the comfort zone when the indoor air movement was 0.4 m/s.

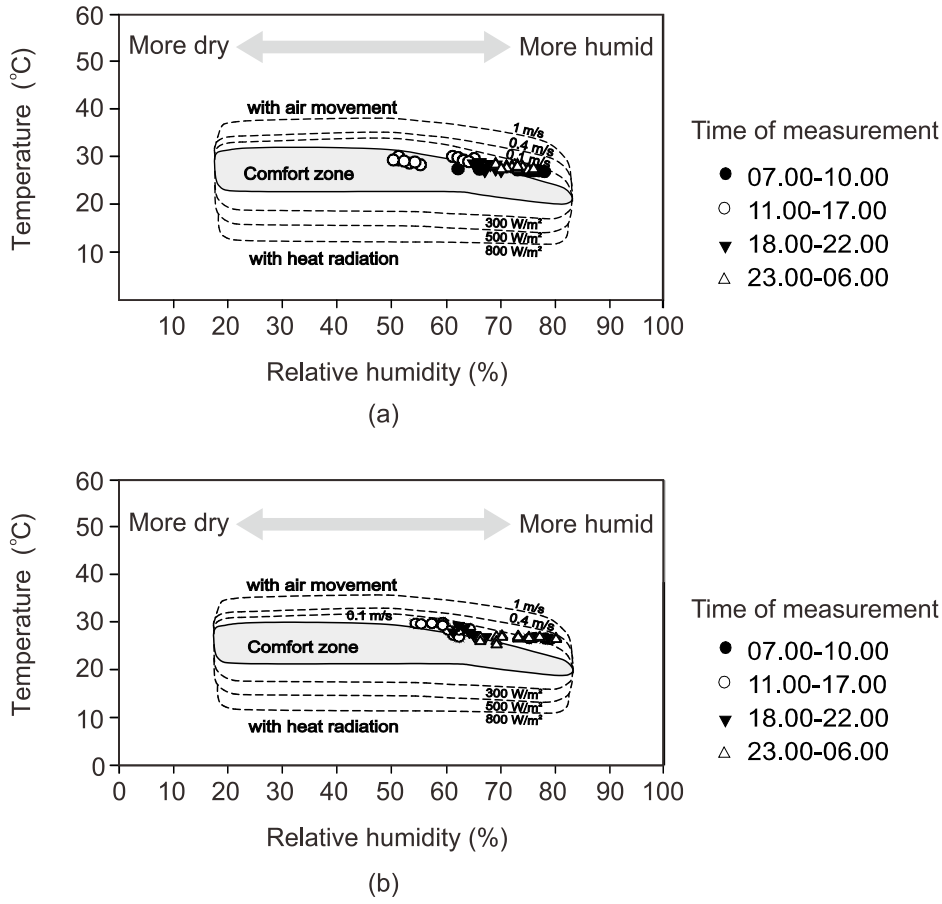


**Fig. 17**. Bioclimatic charts of full-scale house: (a) Scenario 1 (air movement), and (b) Scenario 2 (no air movement)

## 4. Heat transfer finite element analyses

This section studies the effects of convective heat transfer of wall systems, scaled-down house units, and the full-scale house through finite element analyses (FEA). The test results presented in the previous sections are used to calibrate models in Abaqus® to numerically predict the thermal absorption and temperature changes observed in different types of walls. The material and thermal properties of the materials used in the analysis are shown in Table 1. Eight-node hexahedron solid elements were adopted to model the walls and four-node tetrahedron elements were adopted to model the scale down and full-scale houses.

### 4.1. Phase 1: small panel specimens

The 200×200×100 mm wall specimens were modelled in Abaqus®. The finite element (FE) models had fixed supports all around, except at their front and back faces. A temperature of 70°C was then

applied to the front face of the models. The element size was 4mm, as determined by a convergence analysis. The number of elements (62,500) and nodes (83,800) were found after a sensitivity analysis. FEA results for the Mon block and UWall specimens are presented in Fig. 18a and. Fig. 18b, respectively

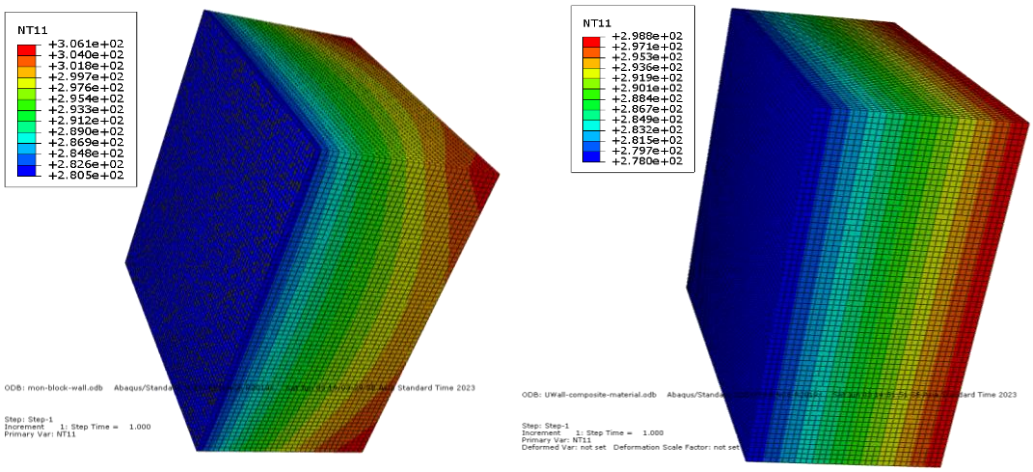


(a) (b)

**Fig. 18.** FEA results of heat transfer analysis (a) Mon block wall w1-c, and (b) UWall specimens w7.

Table 6 compares the FEA and experimental (i.e. sensor RTD3 in Fig. 2a) temperatures, as well as the error percentage between such results. The results in Table 6 indicate that the FE models can predict well the temperatures experienced by the specimens tested in Phase 1. Moreover, the small errors in the FEA predictions (always <5%) in Table 6 indicate that the modelling approach adopted in this study can simulate accurately the thermal behaviour of the different walls. Consequently, the adopted approach is utilised to study the thermal performance of the houses tested in Phases 2 and 3, as described in the following sections.

**Table 6.** Comparison of experimental and FEA results, specimens in Phase 1

| ID | Wall materials | Wall surface finishing | Temperature (°C) | | |
|---|---|---|---|---|---|
| | | | Experimental (RTD3) | FEA | Error |
| w1-c | Mon block wall | Control (no plastering) | 32.7 | 32.9 | 0.6% |
| w2-c | Brick block wall | | 31.2 | 31.5 | 0.9% |
| w3-c | LW block wall | | 30.2 | 28.8 | 4.5% |
| w1-p | Mon block wall | Plastered with mortar | 30.1 | 29.3 | 2.7% |
| w2-p | Brick block wall | | 30.4 | 29.9 | 1.7% |
| w3-p | LW block wall | | 28.7 | 27.7 | 3.6% |
| w4 | Infill wall | Composite wall panel (no plastering) | 28.0 | 27.5 | 1.8% |
| w5 | SIP PU | | 27.0 | 26.8 | 4.6% |
| w6 | SIP EPS | | 26.5 | 27.5 | 0.7% |
| w7 | UWall | | 26.0 | 25.7 | 1.2% |

### 4.2. Phase 2: scaled-down house units (H1 to H7)

3D FE models of the five scale-down house units were also produced in Abaqus®. The element size was 8mm, as determined by a convergence analysis. The number of elements (846,100) and nodes (965,700) were found after a sensitivity analysis. Fig. 19 shows the indoor temperature experienced by the FE model of unit H5, which is representative of the rest of the units. In this case, 70°C heat was applied from the outdoors of the scaled-down houses, and the indoor temperature was recorded. Table 7 compares the temperatures of the five scale-down houses obtained from the FEA and from the tests. It is shown that the FEA predictions agree well with the test results from Scenario 2, with differences always below 8%. These minor differences can be attributed to small variations in indoor temperatures, pressure, air velocity, among others. The FEA results confirm that the use of UWall leads to better thermal comfort compared other walls typically used in houses of Southeast Asia.

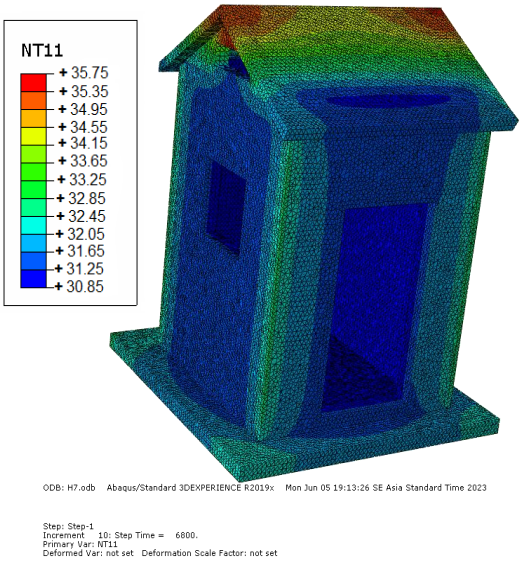


**Fig. 19**. FEA results of indoor temperature (in °C) in scale-down house unit with UWall SIPs (H7).

**Table 7.** Comparison of indoor temperature between tests and FEA results

| ID | Wall materials | Temperature (°C) | | Error |
|---|---|---|---|---|
| | | Test (Scenario 2) | FEA | |
| H1 | Mon block wall | 37.2 | 39.7 | 6.2% |
| H2 | Brick block wall | 37.2 | 36.0 | 3.1% |
| H3 | LW block wall | 36.8 | 33.8 | 8.0% |
| H4 | PU SIP | 37.1 | 37.2 | 0.4% |
| H5 | EPS SIP | 37.0 | 35.9 | 3.6% |
| H6 | Infill wall | 37.1 | 37.3 | 0.6% |
| H7 | U-Wall SIP | 37.0 | 35.7 | 3.4% |

### 4.3. Phase 3: full-scale house (SIP UWall)

### *4.3.1. Numerical study*

The same modelling approach used in the previous section was adopted to model the full-scale house shown in **Fig. 20**. The element size was 10mm, as determined by a convergence analysis. The number of elements (1,350,600) and nodes (1,785,350) were found after a sensitivity analysis. In this case, 70°C heat was applied from the outdoors of the full-scale house, and the indoor temperature was recorded. The highest indoor temperature predicted by the FEA from the second room (refer from Fig 8 and Appendix D) was 30.85°C, which compared very well with the test result of 31°C. The results confirm that the U-Wall can reduce indoor temperature by up to 3°-5°C compared to other typical wall systems because they can reduce the heat flow by storing energy from outdoor space in a hot climate during the day. The FEA results from Abaqus® are generally in good agreement with the experimental test results pointing at the suitability of the software towards analysis of the UWall full-scale house.

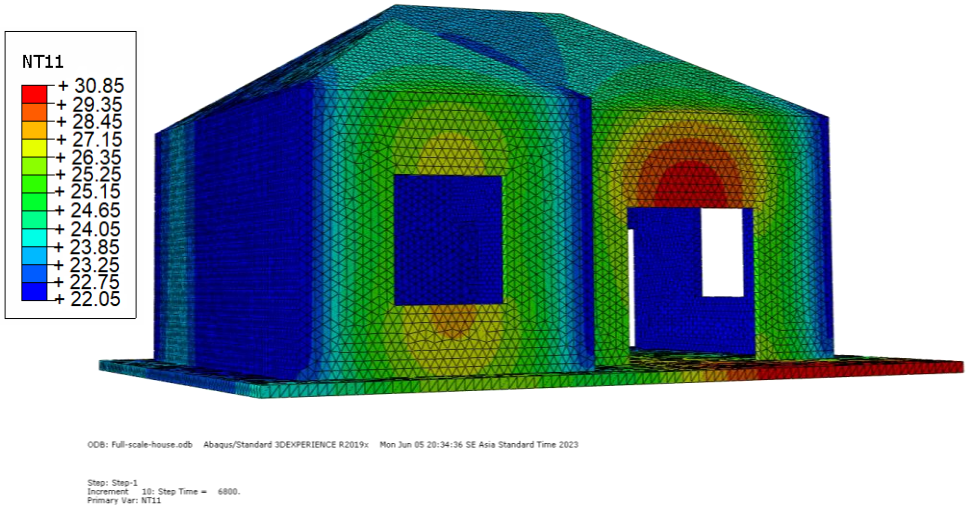


**Fig. 20**. FEA results of indoor temperatures (in °C) for full-scale house

### *4.3.2. Parametric analysis*

A parametric analysis was carried out to provide further insight into the performance of the full-scale house built with UWall SIPs. Different total wall thicknesses ($t_w$ =50 to 250 mm) and different thickness of components ($t_1$ = EPS foam thickness, $t_2$ = EPS foam and foamed concrete, and $t_3$ = cement board thickness) were examined, as reported in **Table 8**. The analysis recorded the indoor temperature on the interior part of the wall (wall inside the house).

**Table 8**. Parametric results of full-scale house with different UWall SIP thicknesses.

| **UWall thickness (mm)** | **Thickness of skin and core materials (mm)** | | | |
|---|---|---|---|---|
| | Cement board | EPS foam | Foamed concrete | Indoor temperature (°C) |
| **50** | 4×2 pcs | 29.50 | 12.5 | 32.87 |
| **75** | 6×2 pcs | 44.25 | 18.75 | 31.43 |
| **100 *** | 8×2 pcs | 59.00 | 25.00 | 30.85 |
| **125** | 10×2 pcs | 73.75 | 31.25 | 27.31 |

| | | | | |
|---|---|---|---|---|
| **150** | 12×2 pcs | 88.50 | 37.50 | 26.55 |
| **200** | 14×2 pcs | 123.63 | 48.37 | 23.47 |
| **250** | 16×2 pcs | 158.76 | 59.24 | 19.83 |

* Original dimensions of UWall SIPs used in Phase 2&3.

Parametric study in **Fig. 21** shows the indoor temperature vs UWall component thickness. The results in this figure suggest that the thickness of EPS foam has the most significant effect for the thermal performance of house. For instance, if the EPS foam $t_2$= 88.5 mm thick, the indoor temperature reduced by 23.8% over the original UWall SIP geometry. Overall, these results highlight the importance of selecting the appropriate thickness of EPS foam for the given thickness of UWall to achieve optimal thermal performance. It should be mentioned that the results presented in **Fig. 21** is only applicable to the UWall SIPs and full-scale house subjected to the atmosphere in the studied area presented in this study. It is also noted that the thickness of the UWall SIP has been optimised to achieve both structural and thermal performance for one storey house subjected to the South-Ease Asia climate. As such, it should not be taken as a general design chart for other case studies.

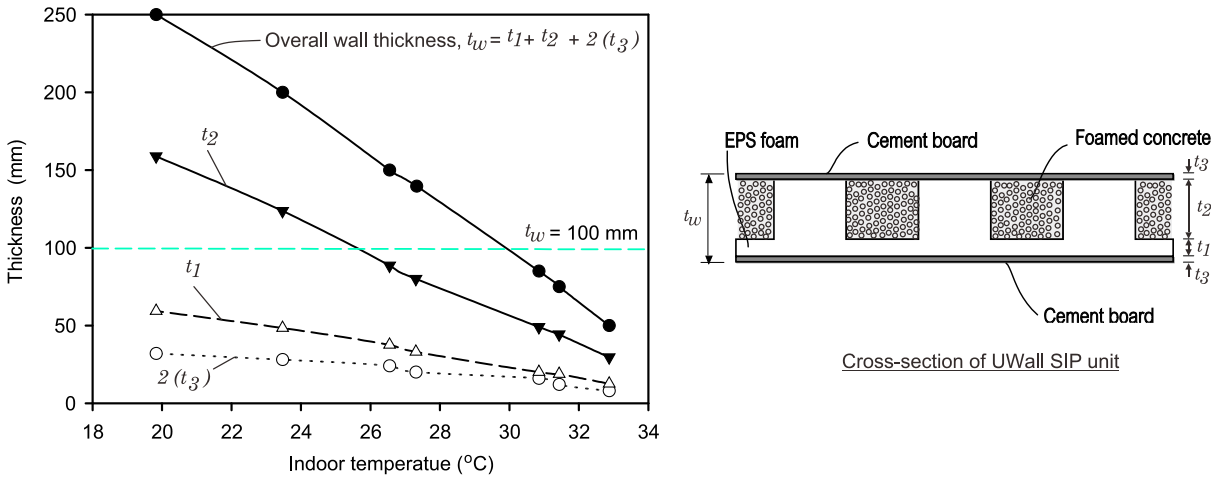


**Fig. 21**. Parametric studs on the influence of skin and core thickness of UWall SIP on indoor temperature.

Based on the experimental test results and FEA simulations presented in this study, it can be concluded that the novel UWall SIPs can be used in the construction of full-scale houses to get a better thermal performance. However, further thermal tests and analysis of structures with other types of wall materials need to be investigated to confirm the findings presented in this study.

## 5. Summary and conclusions

This study investigates the thermal performance of the novel structural insulated panel (SIP) named 'UWall' through diverse tests at different scales and finite element analyses. In Phase 1, 200×200×100 mm block specimens underwent a 12-hour exposure to a temperature of 70°C. Phase 2 involved

constructing five scaled-down (1.5×1.5×2.8 m) house units in Southern Thailand, with continuous monitoring of temperature and relative humidity for 7 days during the summer season. In Phase 3, a 10×7 m full-scale single-storey house was built in Southern Thailand using UWall panels, with simultaneous monitoring of field temperature and humidity, in conjunction with Phase 2 activities. The study delves into the thermal performance of composite wall specimens, seven scaled-down houses featuring different block walls for tropical climates, and a full-scale house.

Based on the presented findings, the following conclusions are drawn:

- In Phase 1, UWall specimens exhibited superior thermal performance compared to other specimens, surpassing mon-block, brick-block, and lightweight-block control specimens, as well as plastered variants, by percentages ranging from 7.6% to 20%. UWall also outperformed other SIPs, including Infill wall, SIP PU, and SIP EPS, by up to 7.6%, 3.8%, and 2%, respectively, owing to its high thermal absorption. Thus, UWall emerges as the optimal choice for achieving superior thermal performance.
- Results from the five scaled-down house units (Phase 2) demonstrated that UWall panels reduced outdoor temperatures by up to 4°C compared to mon-block wall materials. Overall, units constructed with UWall revealed a 15% lower indoor relative humidity (RH) for a given outdoor temperature due to reduced moisture vaporization caused by UWall's heat absorption.
- According to bioclimatic charts, the temperature and humidity within the full-scale house built with UWall panels (Phase 3) exceeded the comfort zone during the daytime, with a temperature difference ranging from 3 to 5°C.
- Finite Element Analysis (FEA) assessed convective heat transfer effects on scaled-down units, the full-scale house, and block specimens. FEA predictions closely aligned with test results (within a 10% accuracy), validating the suitability of the modelling approach.
- A parametric analysis involving seven thermal simulations on the full-scale UWall house led to the proposal of design charts for seven different thicknesses of composite UWall panels. These charts aim to develop a product for achieving significant energy savings in buildings. The results emphasize the crucial role of selecting the appropriate thickness of Expanded Polystyrene (EPS) foam to achieve optimal thermal performance, with a notable instance showing a 23.8% reduction in indoor temperature for an EPS foam thickness (t2) of 88.5 mm compared to the original UWall SIP geometry. Overall, these findings underscore the importance of selecting the right EPS foam thickness for a given UWall thickness to optimize thermal performance.

**Acknowledgements**

The authors also acknowledge the support provided by the Capacity Enhancement and Driving Strategies for Bilateral and Multilateral Cooperation for 2021 (Thailand and UK).

**References**

1. Phanprasit, W.; Rittaprom, K.; Dokkem, S.; Meeyai, A.C.; Boonyayothin, V.; Jaakkola, J.J.K.; Näyhä, S. Climate Warming and Occupational Heat and Hot Environment Standards in Thailand. *Saf Health Work* **2021**, *12*, 119-126. https://doi.org/10.1016/j.shaw.2020.09.008.
2. Nian, V.; Liu, Y.; Zhong, S. Life cycle cost-benefit analysis of offshore wind energy under the climatic conditions in Southeast Asia – Setting the bottom-line for deployment. *Applied Energy* **2019**, *233-234*, 1003-1014, https://doi.org/10.1016/j.apenergy.2018.10.042
3. Katafygiotou, M.C.; Serghides, D.K. Bioclimatic chart analysis in three climate zones in Cyprus. *Indoor and Built Environment* **2014**, *24*, 746-760. https://doi.org/10.1177/1420326X14526909.
4. Gaitani, N.; Mihalakakou, G.; Santamouris, M. On the use of bioclimatic architecture principles in order to improve thermal comfort conditions in outdoor spaces. *Building and Environment* **2007**, *42*, 317-324. https://doi.org/https://doi.org/10.1016/j.buildenv.2005.08.018.
5. Givoni, B. Comfort, climate analysis and building design guidelines. *Energy and Buildings* **1992**, *18*, 11-23, https://doi.org/https://doi.org/10.1016/0378-7788(92)90047-K.
6. Imjai, T.; Phumkesorn, J. Behaviour of Structural Composite Hybrid Panels under Combined Bending and Axial Compression Loads. *Academic Journal of King Mongkut's University of Technology North Bangkok* **2018**, *28*. https://doi.org/10.14416/j.kmutnb.2018.05.002.
7. Ratanawan, T.; Imjai, T.; Israngkura Na Ayudhya, B.; Garcia, R. Experimental study of thermal performance of house models built with conventional or hybrid wall panels. In Proceedings of the International Conference on Sustainable Materials, Systems and Structures (SMSS 2019) Energy Efficient Building Design and Legislation, 2019; pp. 111-116.
8. Kuznik, F.; Virgone, J.; Noel, J. Optimization of a phase change material wallboard for building use. *Applied Thermal Engineering* **2008**, *28*, 1291-1298, https://doi.org/https://doi.org/10.1016/j.applthermaleng.2007.10.012
9. Cui, Y.; Xie, J.; Liu, J.; Wang, J.; Chen, S. A review on phase change material application in building. *Advances in Mechanical Engineering* **2017**, *9*, 1687814017700828, https://doi.org/10.1177/1687814017700828
10. Urgessa, G.; Yun, K.-K.; Yeon, J.; Yeon, J.H. Thermal responses of concrete slabs containing microencapsulated low-transition temperature phase change materials exposed to realistic climate conditions. *Cement and Concrete Composites* **2019**, *104*, 103391, https://doi.org/10.1016/j.cemconcomp.2019.103391 .
11. Baetens, R.; Jelle, B.P.; Gustavsen, A. Phase change materials for building applications: A state-of-the-art review. *Energy and Buildings* **2010**, *42*, 1361-1368,

https://doi.org/10.1016/j.enbuild.2010.03.026

12. Berardi, U.; Gallardo, A.A. Properties of concretes enhanced with phase change materials for building applications. *Energy and Buildings* **2019**, *199*, 402-414, https://doi.org/10.1016/j.enbuild.2019.07.014
13. Socaciu, L.; Plesa, A.; Unguresan, P.; Giurgiu, O. Review on phase change materials for building applications. *Leonardo Electronic Journal of Practices and Technologies* **2014**, 13 (25), 179-194
14. Hawes, D.W.; Feldman, D. Absorption of phase change materials in concrete. *Solar Energy Materials and Solar Cells* **1992**, *27*, 91-101, https://doi.org/10.1016/0927-0248(92)90112-3
15. Rudd, A.F. Phase-change material wallboard for distributed thermal storage in buildings. *ASHRAE Transactions* **1993**, *99*.
16. D'Alessandro, A.; Pisello, A.L.; Fabiani, C.; Ubertini, F.; Cabeza, L.F.; Cotana, F. Multifunctional smart concretes with novel phase change materials: Mechanical and thermo-energy investigation. *Applied Energy* **2018**, *212*, 1448-1461. https://doi.org/10.1016/j.apenergy.2018.01.014.
17. Kalnæs, S.E.; Jelle, B.P. Phase change materials and products for building applications: A state-of-the-art review and future research opportunities. *Energy and Buildings* **2015**, *94*, 150-176, https://doi.org/10.1016/j.enbuild.2015.02.023
18. Ben Romdhane, S.; Amamou, A.; Ben Khalifa, R.; Saïd, N.M.; Younsi, Z.; Jemni, A. A review on thermal energy storage using phase change materials in passive building applications. *Journal of Building Engineering* **2020**, *32*, 101563. https://doi.org/10.1016/j.jobe.2020.101563.
19. Souci, O.Y.; Houat, S. Numerical study of building materials filled by PCM for thermal energy storage. *Epitoanyag - Journal of Silicate Based and Composite Materials* **2018**, *70*, 123-127, https://doi.org/10.14382/epitoanyag-jsbcm
20. Frigione, M.; Lettieri, M.; Sarcinella, A. Phase Change Materials for Energy Efficiency in Buildings and Their Use in Mortars. *Materials (Basel)* **2019**, *12*, https://doi.org/10.3390/ma12081260
21. Jelle, B.P. and Kalnæs, S.E., 2017. Phase change materials for application in energy-efficient buildings. Cost-effective energy efficient building retrofitting, pp.57-118. https://doi.org/10.1016/B978-0-08-101128-7.00003-4.
22. Medina, M.A.; King, J.B.; Zhang, M. On the heat transfer rate reduction of structural insulated panels (SIPs) outfitted with phase change materials (PCMs). *Energy* **2008**, *33*, 667-678, https://doi.org/10.1016/j.energy.2007.11.003
23. Zhang, Y.; Sun, X.; Medina, M.A. Experimental evaluation of structural insulated panels outfitted with phase change materials. *Applied Thermal Engineering* **2020**, *178*, 115454, https://doi.org/10.1016/j.applthermaleng.2020.115454
24. Vinson, J. *The Behavior of Sandwich Structures of Isotropic and Composite Materials* (1st ed.). Routledge 1999. https://doi.org/10.1201/9780203737101.

25. Ryms, M.; Klugmann-Radziemska, E. Possibilities and benefits of a new method of modifying conventional building materials with phase-change materials (PCMs). *Construction and Building Materials* **2019**, *211*, 1013-1024. https://doi.org/10.1016/j.conbuildmat.2019.03.277.
26. Marani, A.; Nehdi, M.L. Integrating phase change materials in construction materials: Critical review. *Construction and Building Materials* **2019**, *217*, 36-49, https://doi.org/10.1016/j.conbuildmat.2019.05.064
27. Fincher, W.; Boduch, M. Standards of human comfort: relative and absolute. 2009.
28. Ormandy, D.; Ezratty, V. Health and thermal comfort: From WHO guidance to housing strategies. *Energy Policy* **2012**, *49*, 116-121, https://doi.org/10.1016/j.enpol.2011.09.003
29. Sassine, E.; Younsi, Z.; Cherif, Y.; Chauchois, A.; Antczak, E. Experimental determination of thermal properties of brick wall for existing construction in the north of France. *Journal of Building Engineering* **2017**, *14*, 15-23. https://doi.org/10.1016/j.jobe.2017.09.007.
30. European Committee for Standardization; British Standards Institution. *Cement: Composition, specifications and conformity criteria for common cements. Part 1*; BSI: 2000.
31. Sun, J.; Yuan, L.; Wang, P. Residual bearing capacity of infilled frame of multi-ribbed composite wall after high temperature. *Construction and Building Materials* **2019**, *214*, 196-206, https://doi.org/10.1016/j.conbuildmat
32. Victor, F.L. Precast Concrete Wall Panels: Design Trends and Standards. *ACI Symposium Publication* **1965**, *11*, https://doi.org/doi:10.14359/16689
33. Cappelletti, F., Gasparella, A., Romagnoni, P. and Baggio, P., 2011. Analysis of the influence of installation thermal bridges on windows performance: The case of clay block walls. Energy and Buildings, 43(6), pp.1435-1442. https://doi.org/10.1016/j.enbuild.2011.02.004
34. Srimuang, K., Imjai, T., Kefyalew, F., Raman, S.N., Garcia, R. and Chaudhary, S., 2023. Thermal and acoustic performance of masonry walls with phase change materials: A comparison of scaled-down houses in tropical climates. Journal of Building Engineering, p.108315. https://doi.org/10.1016/j.jobe.2023.108315
35. Panjehpour, M.; Ali, A.A.A.; Voo, Y.L. Structural Insulated Panels: Past, Present, and Future. *Journal of Engineering, Project & Production Management* 2013, 3(1), 2-8, http://doi.org/10.32738/JEPPM.201301.0002.
36. Eurocode 6. *Design of masonry structures*. British Standard Institution. London. (2005).
37. Kermani, A. Performance of structural insulated panels. *Proceedings of the Institution of Civil Engineers-Structures and Buildings* 159, no. 1 (2006): 13-19. https://doi.org/10.1680/stbu.2006.159.1.13
38. Kermani, A; Hairstans, R. Hairstans, Racking performance of structural insulated panels. *Journal of Structural Engineering*. 2006. 132(11): p. 1806-1812. http://dx.doi.org/10.1061/(ASCE)0733-9445(2006)132:11(1806)

**Appendix A.** Summary of the test results in small panel test in Phase 1.

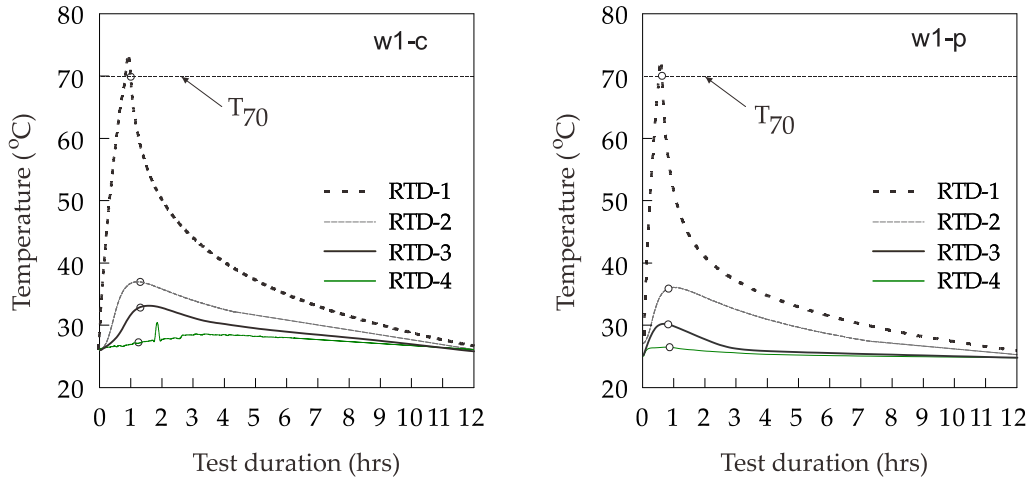


(a) Wall type: mon block

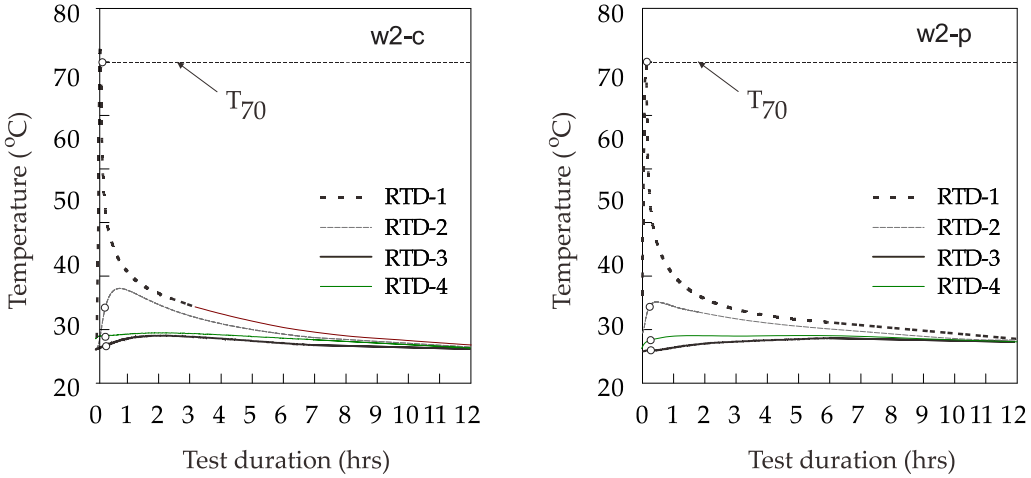


(b) Wall type: brick block

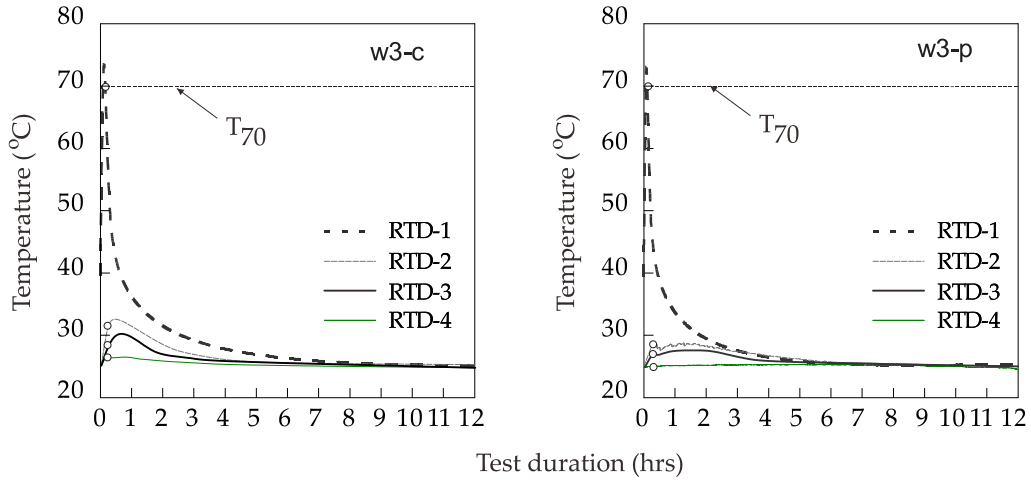


(c) Wall type: Light weight brick

**Fig A.1** Temperature distribution along the wall panel made of conventional materials.

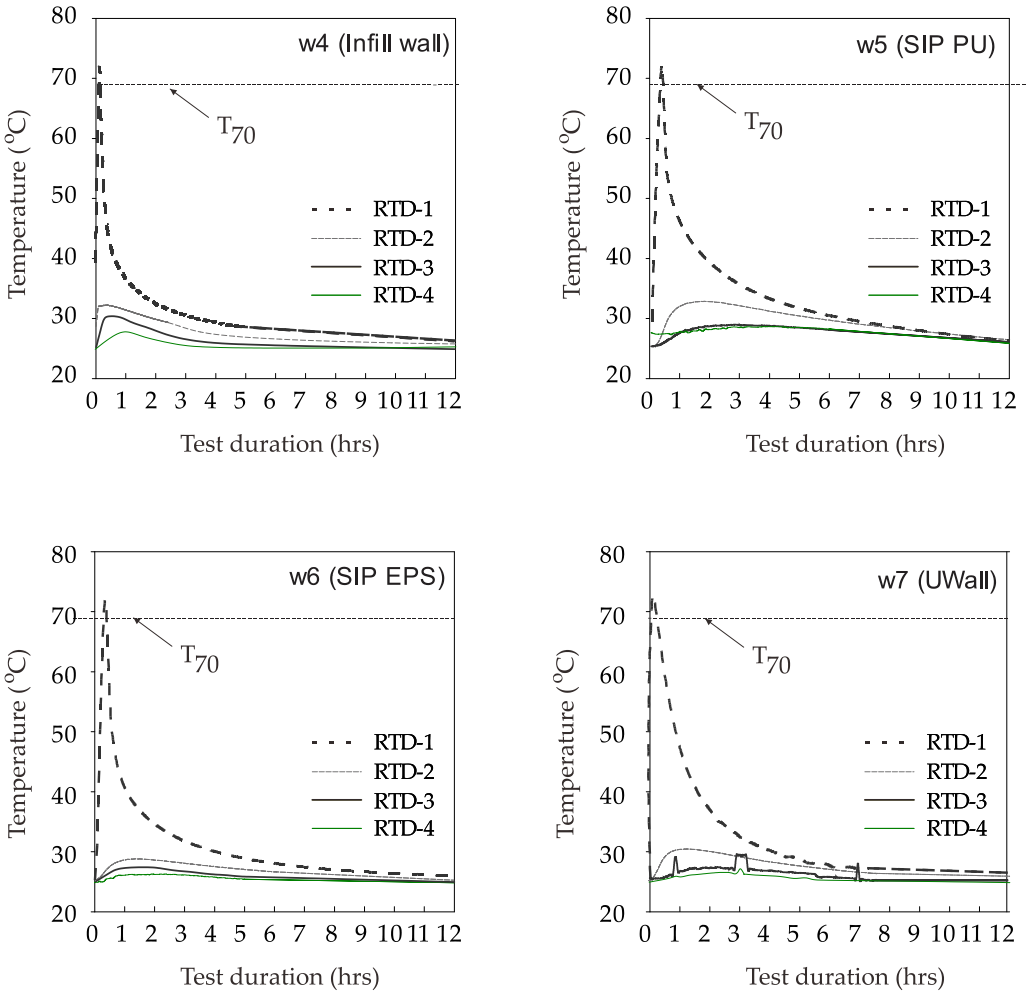


**Fig A.2** Temperature distribution along the wall panel made of composite SIP units.

**Appendix B.**

**Table B-1:** Mean daily temperature and relative humidity (RH) for Chachoengsao Province in year 2019.

| Month | Jan | Feb | Mar | Apr | May | Jun | Jul | Aug | Sep | Oct | Nov | Dec |
|---|---|---|---|---|---|---|---|---|---|---|---|---|
| $T_{m,max}$ | 29.2 | 30.1 | 35.2 | 39.3 | 38.7 | 35.2 | 33.4 | 34.2 | 32.1 | 32.0 | 30.2 | 28.0 |
| $T_{m,min}$ | 17.2 | 18.6 | 32.0 | 33.3 | 32.0 | 29.2 | 28.2 | 25.3 | 27.9 | 26.9 | 24.8 | 15.2 |
| $RH_m$ * | 75.1 | 80.9 | 89.2 | 83.9 | 75.2 | 77.0 | 85.4 | 91.9 | 92.4 | 75.4 | 85.2 | 72.3 |
| $RH_m$ ** | 54.1 | 59.9 | 61.2 | 62.9 | 54.2 | 56.0 | 64.4 | 70.9 | 71.4 | 54.4 | 64.2 | 51.3 |

Note: * measured at 08:00 am ** measured at 14:00 pm.

**Appendix C.** Temperature distribution from numerical analysis

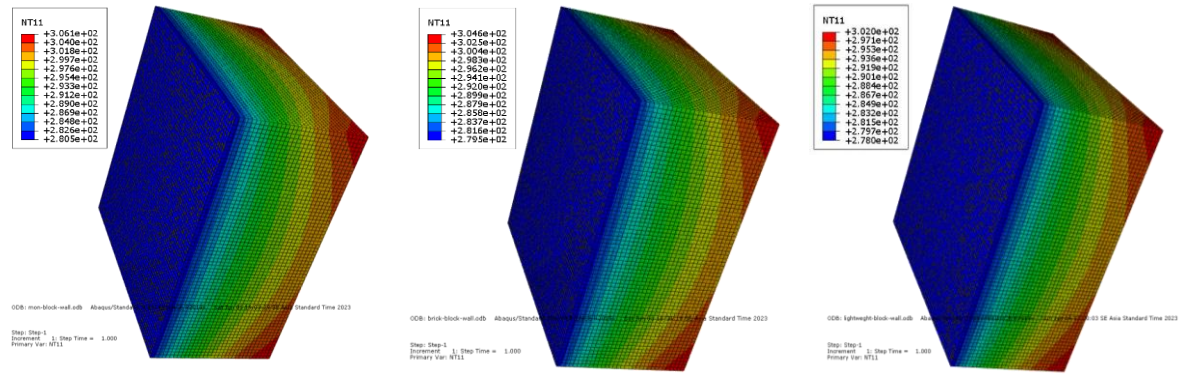

(a) (b) (c)

**Fig C.1.** Typical FEM results of Temperature in Kelvin unit: (a) mon block wall (b) brick block wall, and (c) lightweight block wall.

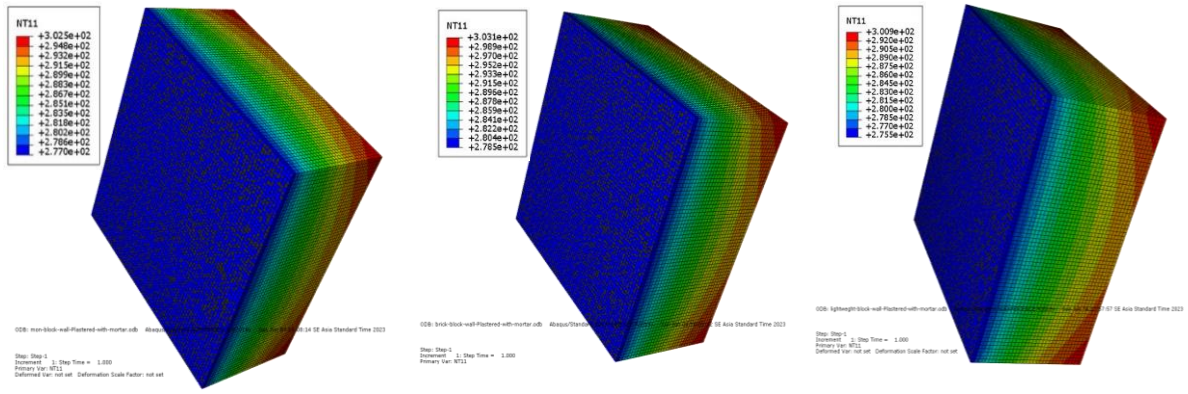

(a) (b) (c)

**Fig C.2.** Typical FEM results of Temperature in Kelvin unit: (a) mon block wall plaster with recycled aggregate mortar (b) brick block wall plaster with recycled aggregate mortar, and (c) lightweight block wall plaster with recycled aggregate mortar.

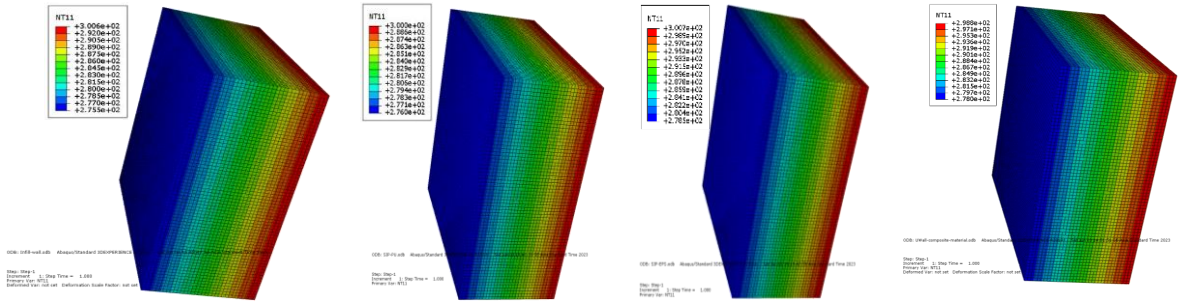

(a) (b) (c) (d)

**Fig C.3.** Typical FEM results of Temperature in Kelvin unit: (a) composite infill wall (b) SIP-PU, (c) SIP-EPS, and (d) composite U-Wall.

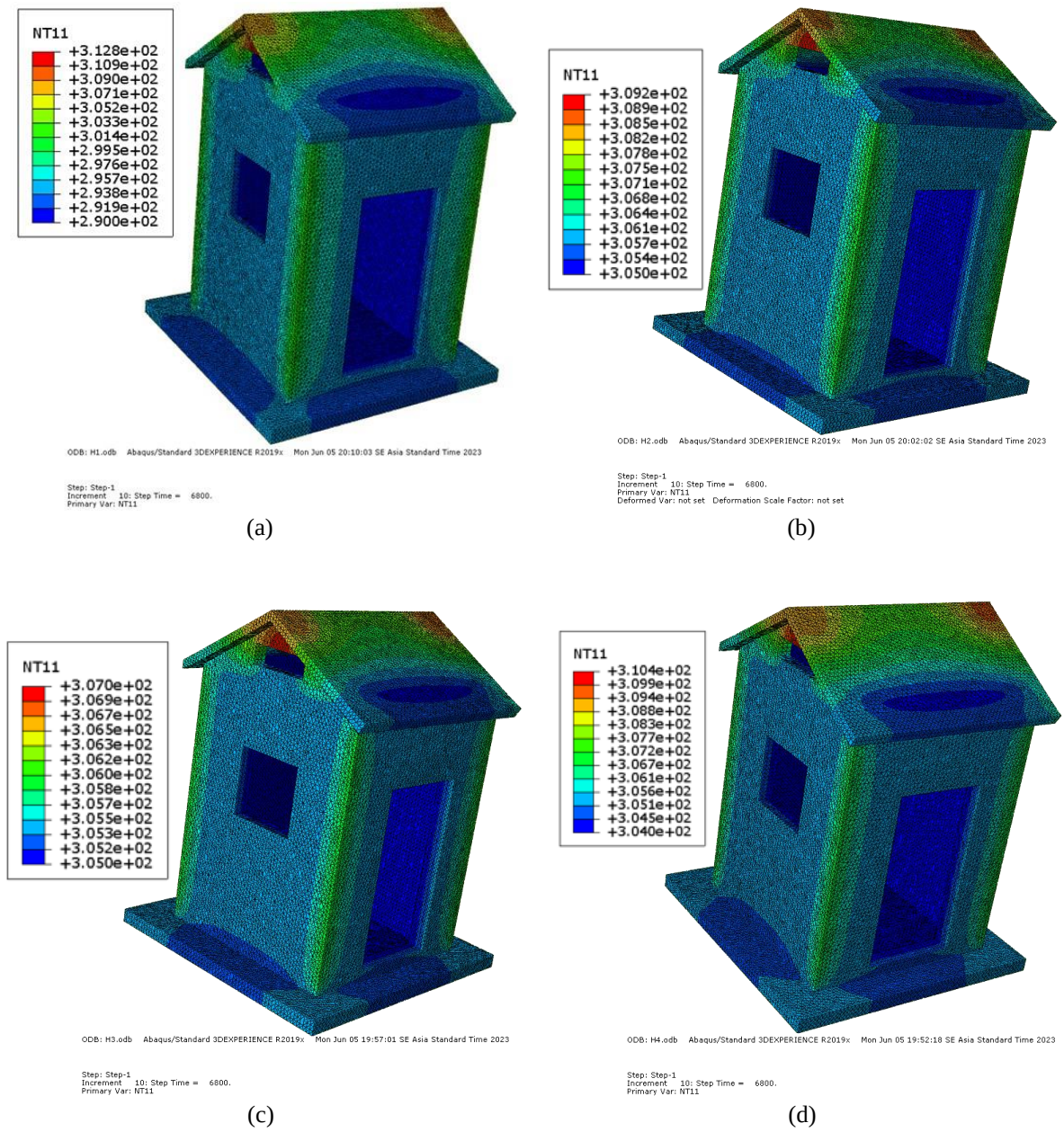


**Fig C.4.** Typical FEM results of Temperature (in $^{o}$K) for Scale down houses build by (a) Mon block wall (b) brick block wall, (c) lightweight block wall, (d) composite infill wall, (e) SIP-PU, (f) SIP-EPS, and (g) composite U-Wall.

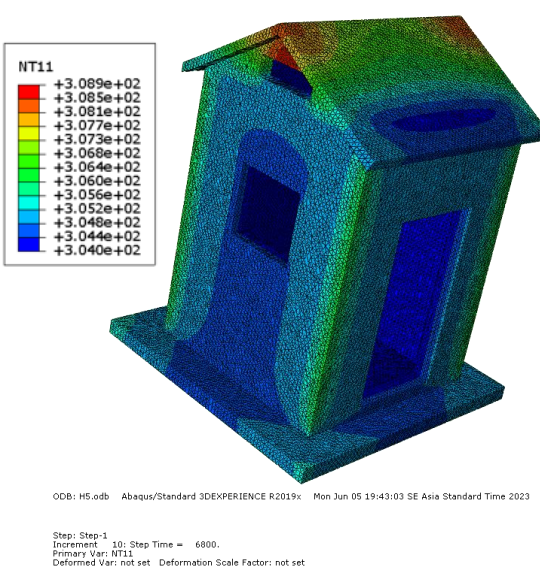


(e)

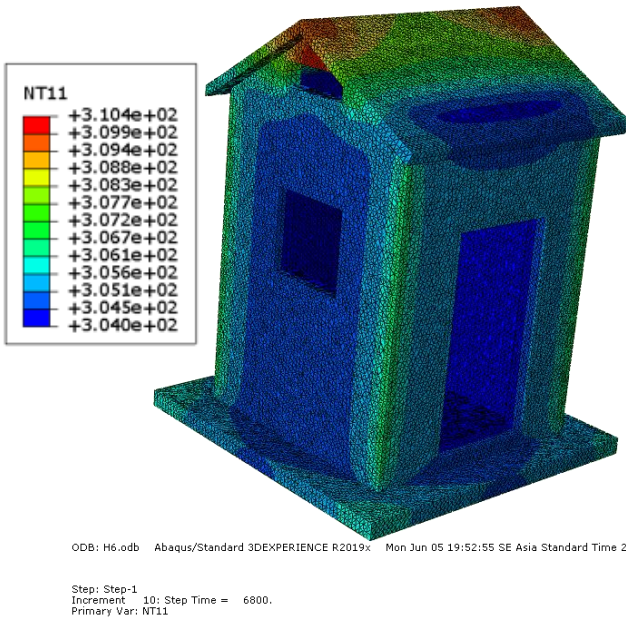


(f)

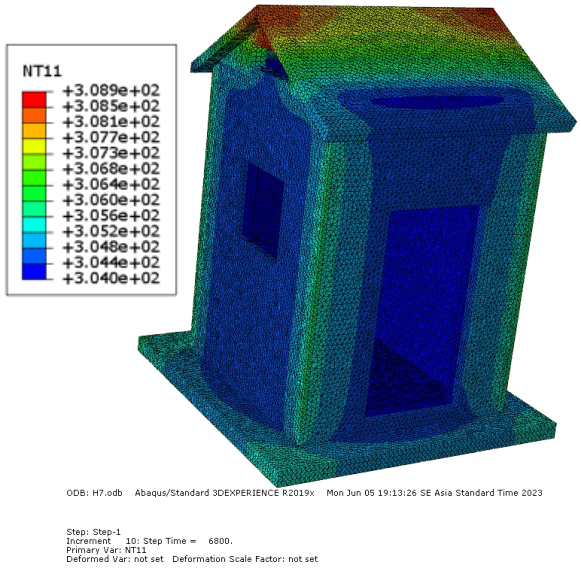


(g)

**Fig C.4.** Typical FEM results of Temperature (in $^{o}$K) for Scale down houses build by (a) Mon block wall (b) brick block wall, (c) lightweight block wall, (d) composite infill wall, (e) SIP-PU, (f) SIP-EPS, and (g) composite U-Wall (cont.).

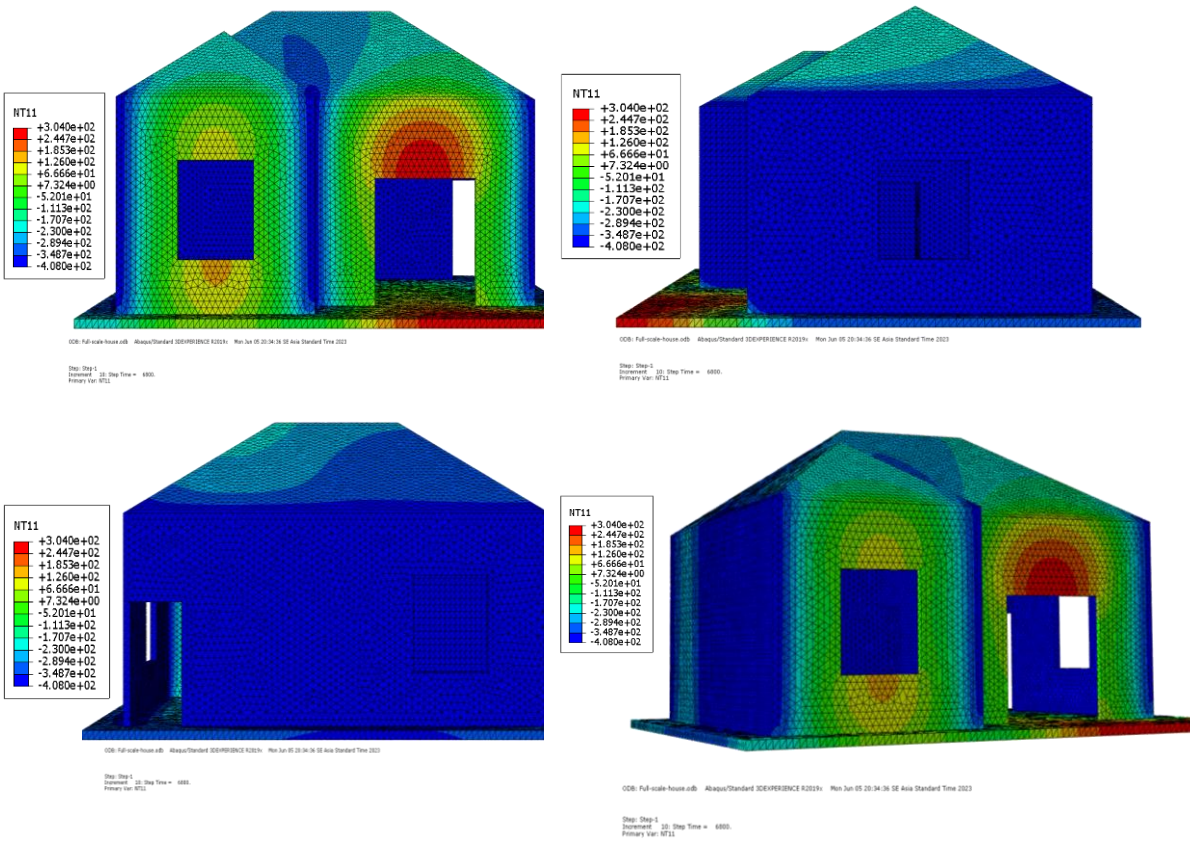


**Fig C.5.** Typical FEM results of Temperature (in $^{o}$K) for full-scale house build by Uwall SIP.

**Appendix D.**

https://youtu.be/cbRH3CAdJKo